

APPLICATIONS OF LANTHANIDE INDUCED SHIFT NMR EXPERIMENTS TO
THE STRUCTURE DETERMINATION OF ORGANIC MOLECULES

A Dissertation

Presented to

the Faculty of the Department of Chemistry

College of Arts and Sciences

University of Houston

In Partial Fulfillment

of the Requirements for the Degree

Doctor of Philosophy

by

Robert Lenkinski

August 1973

703628

TO LOUIS, HELEN AND LIONEL

ACKNOWLEDGEMENT

For the period of my graduate education 1969 to 1973, I have had the rare privilege of working with Professor M. Robert Willcott III. His examples both as a research chemist and as a teacher provide me with a goal and inspiration for my career. I am grateful for his interest and encouragement in this work.

I am deeply indebted to Dr. James R. Cox, Jr. who provided a guiding light in times of darkness. He will serve as an inspiration to me. Professor Jerry M. Fitzgerald, through personal friendship and scientific discussion, has also left his impact on my education. Dr. Ray E. Davis is in no small way responsible for this work. I thank him for his interest and stimulation. His contribution to this work is the development of a computational method, without which, much of this work would be meaningless. I would like to thank Paul A. Loeffler and Dr. Otto A. Gansow for their contribution to this work. Without their help much of the carbon-thirteen work would have been impossible.

Of my fellow graduate students Roger Knapp, Mike Rathburn, Pat Howard and Walter Waddell must be recognized for their helpful criticism and for their personal friendship.

Mrs. Sherry Simmons is to be commended for her patience in helping me prepare this manuscript.

APPLICATIONS OF LANTHANIDE INDUCED SHIFT NMR EXPERIMENTS TO
THE STRUCTURE DETERMINATION OF ORGANIC MOLECULES

An Abstract of
A Dissertation
Presented to
the Faculty of the Department of Chemistry
College of Arts and Sciences
University of Houston

In Partial Fulfillment
of the Requirements for the Degree
Doctor of Philosophy

by
Robert Lenkinski
August 1973

ABSTRACT

The problem of using lanthanide induced shift (LIS) data to determine the structure of organic molecules is attacked by considering the following topics.

- I. How can LIS indices best be determined?
- II. Should the observed shifts be factored into contact and pseudocontact contributions?
- III. Is the use of the McConnell-Robertson relationship for axially symmetric ions appropriate?
- IV. What orientation of the principal magnetic axis should be used for the computer simulation of the experiment?
- V. What is the optimum method for matching experimental and calculated LIS values?

The results of five methods of determining LIS indices for pyridine and THF are compared. Although the absolute magnitudes of the LIS indices vary from method to method, the set of internally scaled LIS indices are virtually identical.

A computational method is developed which is based on the McConnell-Robertson pseudocontact relationship for axially symmetrical ions. An assessment of how well a set of experimental LIS indices fits a given substrate topology is furnished by the agreement factor, R.

$$R = \left[\frac{\sum_i ((\Delta H/H)_{oi} - (\Delta H/H)_{ci})^2 w_i}{\sum_i (\Delta H/H)_{oi}^2 w_i} \right]^{1/2} *$$

This agreement factor is the same R factor used in X-ray crystallography and can be used in statistical hypothesis testing.

The computational method is shown to replicate almost all ^1H LIS data very well. Attempts to use the McConnell-Robertson relationship to replicate ^{13}C -Eu(DPM)₃ data result in large discrepancies between observed and calculated LIS values. In an attempt to find a shift reagent which produces shifts consistent with the McConnell-Robertson relationship, isoquinoline LIS data for eight lanthanide shift reagents were fitted against the pseudo-contact relationship. The best agreement was found for Yb(DPM)₃.

Applications of the computational method to nitrile containing substrates are explored. Examples of the use of LIS data to determine conformations in solution are presented.

*For details see M. R. Willcott III, R. E. Lenkinski and R. E. Davis, J. Amer. Chem. Soc., 94, 1742 (1972).

TABLE OF CONTENTS

	Page
DEDICATION.	i
ACKNOWLEDGEMENT	ii
ABSTRACT	iii
LIST OF FIGURES	x
LIST OF TABLES	xi
CHAPTER I. HISTORICAL BACKGROUND	1
CHAPTER II. STATEMENT OF PURPOSE.	5
CHAPTER III. THE LSR-SUBSTRATE COMPLEX	7
The Lanthanide Shift Reagent (LSR)	7
Substrates	12
The Dynamic Nature of the LSR-Substrate Association.	13
CHAPTER IV. AN EVALUATION OF THE VARIOUS DATA TREATMENT TECHNIQUES	17
The Stoichiometry of the LSR-Substrate Interaction.	18
Experimental Variation of the Induced Shift with LSR/Substrate Concentration.	20
Algebraic Formulation of the Various LIS Data Refinement Methods.	22
Demarco Method	23
A Rigorous Method.	24

TABLE OF CONTENTS CONTINUED

	Page
Willcott-Herndon-Lenkinski Method	25
Kelsey Method	25
ApSimon Method.	26
Summary of Various Data Work-Up Schemes	26
Experimental Procedure	28
(1) Tetrahydrofuran (THF) - Eu(DPM) ₃	
in CCl ₄	28
(2) Pyridine-Eu(DPM) ₃ in CCl ₄	29
(3) Pyridine - Pr(DPM) ₃	29
A Comparison of the Results of the Five	
Methods of Data Treatment in Lanthanide	
Induced Shift Experiments	30
CHAPTER V. CONSTRUCTION OF THE MODEL FOR THE LSR-	
SUBSTRATE INTERACTION	38
A. Theoretical Considerations	38
δ_{contact}	39
$\delta_{\text{pseudocontact}}$	39
Justification of the Pseudocontact	
Model for ¹ H LIS Data	42
The Question of Axial Symmetry	45
The Question of the Orientation of	
the Principal Magnetic Axis	48

TABLE OF CONTENTS CONTINUED

	Page
B. The Mathematical Model for the LSR-Substrate Interaction.	50
Significance Testing on the Agreement Factor, R	58
CHAPTER VI. APPLICATIONS OF THE PSEUDOCONTACT MODEL	
TO LIS EXPERIMENTS	61
A. Extension of the Computational Method to ^{13}C LIS Spectra	61
Discrepancies in $\text{Eu}(\text{DPM})_3$ - ^{13}C Spectra.	61
The Evaluation of Lanthanide Induced Carbon-13 Contact <u>vs</u> Pseudo- contact NMR Shifts	71
<u>endo</u> -Norborn-5-en-2-ol.	78
3-Fluoropyridine.	82
B. "Collinearity in the Structural Elucidation of Nitriles"	85
Doering's Feist's Acid Derivatives.	85
Methylacrylonitriles	86
Cyanocyclopropane	94
Benzonitriles.	94

TABLE OF CONTENTS CONTINUED

	Page
Conformational Analysis Using	
Nitrile-Containing Compounds.	97
CHAPTER VII. SUMMARY OF THE COMPUTATIONAL METHOD.	104
BIBLIOGRAPHY	107
APPENDIX A Eu(DPM) ₃ LIS DATA FOR SOME RIGID BICYCLIC	
OXYGENATED HYDROCARBONS.	114
The General Experimental Procedure for	
Obtaining ¹ H LIS Indices	114
5-Methylbicyclo[3.2.0]hept-3-en-2-one	115
Bicyclo[3.2.0]hept-3-en-2-one.	115
Borneol	118
Isoborneol	118
Norcamphor	118
<u>endo</u> -Norborn-5-en-2-ol	119
The Experimental Procedure for Determining	
the ¹³ C LIS Indices for Borneol	120
Borneol ¹³ C LIS Data.	120
Isoborneol ¹³ C LIS Data.	120
APPENDIX B GENERAL PROCEDURE FOR OBTAINING A SET OF	
MATCHED ¹³ C AND ¹ H LIS INDICES FOR A	
COMPOUND	121

TABLE OF CONTENTS CONTINUED

	Page
APPENDIX C ^1H Yb(DPM) ₃ -LIS DATA FOR SOME NITRILE CONTAINING SUBSTRATES	123
General Experimental Procedure for Obtaining ^1H Yb(DPM) ₃ -LIS Data for Nitrile Containing Substrates	123

LIST OF FIGURES

	Page
1. The Proton NMR Spectra of Both Cholesterol and Cholesterol in the Presence of $\text{Eu}(\text{DPM})_3$	4
2. Variation of the Observed Shift for the H_2 Resonance of Borneol with the Mole Ratio of $\text{Eu}(\text{DPM})_3$ /- Borneol	21
3. A Graphical Definition of r , θ and Ω , the Variables Described in the McConnell-Robertson Expression	41
4. The Orientation of the Principal Magnetic Axis in the LSR-Substrate Complex	49
5. <u>endo</u> -Norbornenol as Described with Respect to the Internal Coordinate System	55
6. Plots of the Agreement Factor R for <u>endo</u> -Norbornenol	56
7. The Observed and Calculated $\text{Yb}(\text{DPM})_3$ Indices for 3-Fluoropyridine	83
8. The Observed and Calculated $\text{Eu}(\text{DPM})_3$ Indices for 3-Fluoropyridine	84
9. The Observed $\text{Yb}(\text{DPM})_3$ -Proton Indices for Four Substituted Benzonitriles with Agreement Factors for Each	96
10. The Observed $\text{Yb}(\text{FOD})_3$ - ^1H Indices for <u>Cis</u> and <u>Trans</u> -1-Cyano-2-Vinylcyclobutane Determined by Doering.	98
11. Variation of the Agreement Factor, R, with Ring Pucker in the Cyclobutyl Ring of <u>Cis</u> -1-Cyano-2-Vinylcyclobutane	99
12. Variation of the Agreement Factor, R, with the Ring Pucker in the Cyclobutyl Ring of <u>Trans</u> -1-Cyano-2-Vinylcyclobutane	100
13. Variation of the Agreement Factor, R, with the Conformation of the Vinyl Group for each of the Olefinic Resonances of <u>Trans</u> -1-Cyano-2-Vinylcyclopropane	102

LIST OF TABLES

	Page
I. Isotropic Shift Data for 4-Vinylpyridine and Line-Width Data for 2-Picoline Adducts of $\text{Ln}(\text{DPM})_3$	9
II. Some Functional Groups which have been Reported to Interact with LSRs	14
III. A Summary of the Various Techniques of Data Treatment in Lanthanide Induced Shift (LIS) Experiments	31
IV. A Comparison of the Shift Indexes Computed by Five Different Methods on THF-Eu(DPM) ₃ and Pyridine Eu(DPM) ₃ Data	33
V. A Comparison of the Shift Indexes Computed by Five Different Methods on Pyridine-Pr(DPM) ₃ Data	34
VI. Relative Contact Shifts for Nuclei in the Same Molecule and of the Same Fractional Spin Occupancy	43
VII. Minimum Agreement Factors Obtained for Oxygenated Hydrocarbons	53
VIII. Comparison of Observed and Calculated Lanthanide-Induced Chemical Shifts for the System: Eu(DPM) ₃ -endo-Norborn-5-en-2-ol	54
IX. Experimental 1:1 Eu(DPM) ₃ -Substrate Chemical Shifts of Some Pyridine Bases	68
X. Observed and Calculated 1:1 ¹ H and ¹³ C LIS Indices for Isoquinoline with Eight Lanthanide Shift Reagents.	70
XI. Minimum Proton R Factors, Lanthanide Nitrogen Distances, and Combined ¹³ C-H R Factors.	74
XII. ¹³ C Difference Spectra for the Nitrogen Ring of Isoquinoline	75
XIII. Average Values for $\delta_{\text{pseudocontact}}/\delta_{\text{contact}}$ in the Nitrogen Ring of Isoquinoline for Eight Different Lanthanides	77

LIST OF TABLES CONTINUED

	Page
XIV. Experimental and Calculated ^1H and ^{13}C Eu(DPM) $_3$ and Yb(DPM) $_3$ LIS Indices for <u>endo</u> -Norborn-5-en-2-ol	79
XV. Minimum Agreement Factors and Lanthanide Positions for ^{13}C and ^1H LIS Indices of <u>endo</u> -Norborn-5-en-2-ol	81
XVI. Chemical Shifts and Observed and Calculated Relative Slopes, Compounds 1-4 with Eu(FOD) $_3$	87
XVII. Minimum R Values (%) for Binary Combinations of Models 1-4 with Sets of Relative Slopes, No Restraint of Lanthanide Position	88
XVIII. Minimum R Values (%) for Binary Combinations as in Table XVII, with Collinearity Restraint	90
XIX. Chemical Shifts and Observed and Calculated Relative Slopes, Methylacrylonitrile:Yb(DPM) $_3$, with Collinearity Restraint	91
XX. Minimum R Values (%) and Lanthanide Positions for Binary Combinations of Methylacrylonitrile Models 5-7 with Sets of Relative Slopes, no Restraint of Lanthanide Position	92
XXI. Minimum R Values (%) for Binary Combinations of Methylacrylonitrile Models 5-7 with Sets of Relative Slopes, with Collinearity Restraint	93
XXII. The Variation of the Agreement Factor, R, with the Lanthanide Position for the Cyanocyclopropane ^1H -Yb(DPM) $_3$ System	95
XXIII. Experimental Eu(DPM) $_3$ LIS Data for 5-Methylbicyclo[3.2.0]hept-3-en-2-one	116
XXIV. Experimental LIS Data for Bicyclo[3.2.0]hept-3-en-2-one	117
XXV. ^1H Yb(DPM) $_3$ -LIS Data for Structure I	124
XXVI. ^1H Yb(DPM) $_3$ -LIS Data for Cyanocyclopropane	125

CHAPTER I
HISTORICAL BACKGROUND

I. HISTORICAL BACKGROUND

Recent advances in nuclear magnetic resonance spectroscopy have involved either the modification of instrumental design or the sophistication of computer data refinement techniques. The more spectacular of these advances have been the development of superconducting magnets, which have brought about a tremendous increase in the magnetic field strength, and the application of Fourier-transform techniques to pulsed NMR experiments, which have increased the sensitivity of the NMR experiment appreciably. The result of these advances has been an increase in the number of kinds of experiments available to chemists. Unfortunately these successful techniques usually bear large price tags. It should come as no surprise therefore, that a widely applicable, easily understood, low-cost, chemical method of spectral alteration, which was recently reported in the chemical literature, has created such excitement in NMR research.

The first report in 1969, by Hinckley¹, that certain lanthanide- β -diketonates could be used to facilitate spectral analysis, has stimulated a flood of reports dealing with both the methodology and the applications of "shift reagents". However the use of metal ions to alter NMR spectra began earlier than 1969. In 1960, Taube and co-workers² used the shifts induced by the presence of Co(II) ion to study the hydration spheres of the diamagnetic salts of Be(III), Al(III) and Ga(III). The addition of Co(II) ion to an aqueous solution of the various diamagnetic salts resulted in the observation of two extremely broad resonances in the oxygen-17 NMR spectra of each salt.

The authors assigned the resonances to the waters of hydration of the diamagnetic ion and to the solvent water. The shift induced in the solvent water resonance was rationalized by a rapid exchange between the solvent water molecules and the waters molecules in the hydration sphere of Co(II) ion. In 1963, Connick and Fiat³ measured the relative areas of these two oxygen-17 resonances in the same system. From these measurements, the hydration numbers of the diamagnetic ions were determined. The authors noted that the extreme line broadening observed with Co(II) ion caused considerable difficulty in determining the relative areas of the two peaks accurately.

In 1965, Taube and coworkers⁴ investigated the oxygen-17 NMR spectra of aqueous solutions of paramagnetic lanthanide ions. In all cases except gadolinium, line broadening was either very small or not observed. This lack of line broadening led Taube to the conclusion that the rare earth ions were better "shift reagents" for hydration studies.

In 1957, Phillips, Looney and Ikeda⁵ used Co(II) ion to alter the proton spectra of n-propanol and n-hexanol. In 1963, Eaton, Josey, Phillips and Benson⁶ used shifts induced by nickel(II) in nickel(II) aminotroponeiminates to simplify the proton spectrum of the aminotroponeiminate which facilitated the measurement of various spin-spin coupling constants. In 1965, Eaton⁷ found shifts induced in the proton resonances of the acetylacetonate chelates of various transition metals and of several lanthanides. Also in 1965, Muettterties and Wright⁸ reported large shifts induced in the proton resonances of the rare earth tris-tropoloneates.

In 1969, Hinckley¹ reported that the addition of the dipyridine adduct of tris-divaloylmethanato-europium(III) to a dilute solution of cholesterol monohydrate, in carbon tetrachloride, caused a dispersion of the proton resonances in cholesterol. Figure 1 shows two spectra. The first spectrum is the spectrum of a .1M solution cholesterol in carbon tetrachloride. The second spectrum is the spectrum of cholesterol altered by the addition of .05M of $\text{Eu}(\text{DPM})_3 \cdot 2\text{py}$. An inspection of these two cholesterol spectra and the rest of Hinckley's report leads to the following observations.

1) There is only one set of shifted resonances in the "perturbed" cholesterol spectrum.

2) The structurally closer a given proton is to the hydroxyl function, the more it seems to be shifted by the addition of $\text{Eu}(\text{DPM})_3 \cdot 2\text{py}$.

3) The more $\text{Eu}(\text{DPM})_3 \cdot 2\text{py}$ is added the greater the "perturbation" in the cholesterol spectrum. Clearly, any attempts to rationalize the results of lanthanide induced shift (LIS) experiments must be developed in such a way as to be consistent with these three observations.

FIGURE 1: THE PROTON NMR SPECTRA OF BOTH CHOLESTEROL AND
CHOLESTEROL IN THE PRESENCE OF $\text{Eu}(\text{DPM})_3$
(From reference 1)

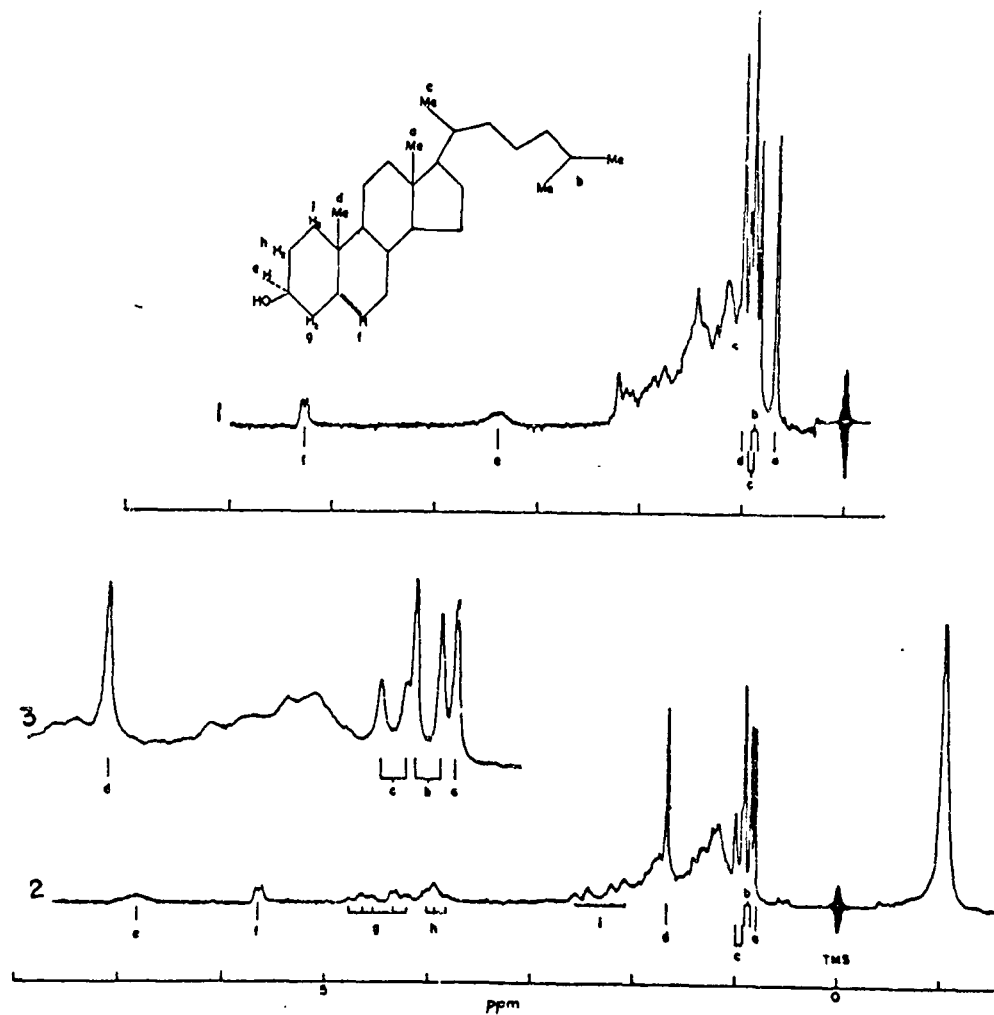


Figure 1. Spectrum 1 is of cholesterol monohydrate in CCl_4 . Spectrum 2 is of a CCl_4 solution 0.05 M in $\text{Eu}(\text{DPM})_2 \cdot 2\text{py}$ and 0.1 M in cholesterol monohydrate. Spectrum 3 is an expansion of that region of spectrum 2 which includes the methyl resonances. Assignments are indicated by letter on the accompanying molecular diagram. The resonance 1 ppm upfield from tetramethylsilane (TMS) is due to the metal complex.

CHAPTER II
STATEMENT OF PURPOSE

II. STATEMENT OF PURPOSE

The approach that we will follow in this thesis on lanthanide induced shift (LIS) experiments in NMR, will be to answer the questions "Can we determine the structure of organic molecules from their LIS data?" by considering the following discrete questions.

1) Is there a description of the lanthanide shift reagent (LSR) substrate association which is chemically sensible?

2) Can the mathematical methods used to refine the set of perturbed LIS spectra into a set of LIS indices be evaluated to find the most convenient method for determining these LIS indices.

3) Can a model for the lanthanide shift reagent substrate interaction be developed which takes the set of LIS indices from question 2 and matches them against a given lanthanide shift reagent-substrate topology*.

It is our goal to develop a mathematical method, which, when applied to a given set of LIS data and either a single structure, or a set of structures, furnishes an assessment of how well that data set matches any of the given structures. We propose to use LIS data for simple molecules of known structure to construct and test our proposed model. When our method of analysis can be shown to select only the structures consistent with other chemical information, then we will apply our method to LIS data for molecules of undetermined structure.

*Topology should be taken to mean internal substrate structure as well as the spatial orientation of the substrate with respect to a LSR molecule.

It is important to stress, at this point, that the criterion for the merit of any proposed model will be whether the structures predicted by that method match only the real structures of the molecules under investigation.

CHAPTER III
THE LSR-SUBSTRATE COMPLEX

III. THE LSR-SUBSTRATE COMPLEX

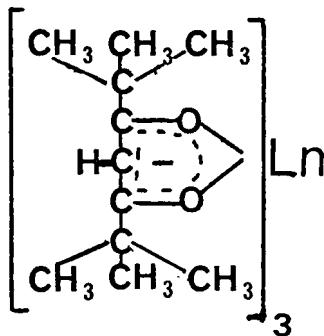
There are two questions that arise about the LSR-substrate complex.

- 1) What is the chemical rationalization for the LSR-substrate bond formation?
- 2) Is the LSR-substrate complex a static or dynamic system?

The first question can best be answered by examining both the nature of the LSRs and the nature of the substrates which interact with LSRs.

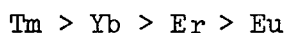
The Lanthanide Shift Reagent (LSR)

The shift reagents most commonly used are the tris- β -diketonates chelate of the lanthanide in their (III) oxidation state. The lanthanide metals in the anhydrous form of these chelates are hexacoordinate. One of the β -diketone ligands commonly used is 2,2,6,6-tetramethyl-3,5-heptanedione (HDPM). A two dimensional representation of the structure of the HDPM chelates is shown below.



The synthesis of these chelates was carried out by Sievers⁹ and coworkers. The chelates are crystalline substances which are

reported to be slightly hygroscopic. The $\text{Ln}(\text{DPM})_3$ compounds are fairly soluble in most common solvents used in NMR. For example, about 70 mg $\text{Eu}(\text{DPM})_3$ is soluble in 0.5 ml of carbon tetrachloride. The solubility of these HDPM LSR's increases in the presence of suitable organic substrates. (Suitable substrates will be described in the next section.) The relative shifting abilities of the $\text{Ln}(\text{DPM})_3$ LSRs were reported by Horrocks and Sipe.¹⁰ These results along with line broadening data for each lanthanide are shown in Table I. Note that the chelates of Eu, Yb, Tm and Er shift proton resonances downfield while Pr, Nd, Tb, Dy and Ho all shift proton resonances upfield. Ordering the downfield shifting lanthanides in terms of their relative shifting ability, we see the following order.



Ordering the same lanthanide in terms of their line broadening characteristics, we find



Ordering the upfield shifting lanthanides in terms of their shifting ability we see,



Ordering the same lanthanides in terms of their line broadening characteristics we find,

TABLE I^(c)

ISOTROPIC SHIFT DATA FOR 4-VINYLPYRIDINE AND LINE-WIDTH
DATA FOR 2-PICOLINE ADDUCTS OF $\text{Ln}(\text{DPM})_3$

Ln	Observed H-2 isotropic shift, ppm ^(a)	$\Delta\nu_{1/2}$ ^(b) Hz
Pr	+6.6	5.6
Nd	+3.2	4.0
Sm	+0.8	4.4
Eu	-3.5	5.0
Tb	+30.7	96
Dy	+33.8	200
Ho	+24.0	50
Er	-9.1	50
Tm	-23.6	65
Yb	-11.0	12

(a) Observed for LSR-substrate mole ratio = 0.125.

(b) Width at half maximum for the methyl resonance of 2-picoline.

(c) From Reference 10.

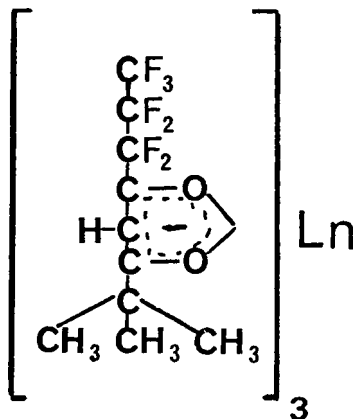
Dy > Tb > Ho > Pr > Nd > Sm

In choosing a particular lanthanide for an experimental application, considerations of both the relative line broadening characteristics and relative shifting ability must be made.

Horrocks, Sipe and Luber¹¹ have determined the crystallography of the bis-4-picoline adduct of $\text{Ho}(\text{DPM})_3$, by X-ray. In the crystal, the Ho atom was found to be eight coordinate, with a nearly square antiprismatic coordination polyhedron. The only axis of symmetry in the crystalline structure was found to be a C_2 axis bisecting one of the three chelate rings*. The Ho-N bond distance was reported to be 2.53Å, which compares to the 2.65Å Ln-N bond distance reported in $\text{La}(\text{NO}_3)_3 \cdot 2\text{py}$.¹² Horrocks notes that the crystal structure may not necessarily be maintained in dilute solution. That is, the symmetry of these LSRs in the NMR experiment may be different than the symmetry of the LSRs in their crystalline form. The nonrigidity of the tris-tropolanate lanthanide chelates in solution has been reported by Muetterties and Wright.¹³ Randall¹⁴ et al. and Marshall¹⁵ et al. have noted that the LSR-substrate complex is not necessarily a rigid system in solution.

Another ligand commonly used is 1,1,1,2,2,3,3-heptafluoro-7,7-dimethyl-4,6-octanedione (HFOD). A two dimensional representation of the structure of this type of chelate is shown on the next page.

*This point is very important and will be discussed more fully in a later chapter.



The synthesis of the HFOD chelates of the lanthanide has been carried out by Sievers and co-workers.¹⁶ These authors reported that the $\text{Ln}(\text{FOD})_3$ chelates are more soluble than the corresponding $\text{Ln}(\text{DPM})_3$ chelates in most organic solvents.* The $\text{Ln}(\text{FOD})_3$ chelates are also reported to exhibit greater Lewis acidity than the corresponding $\text{Ln}(\text{DPM})_3$ chelates. The $\text{Ln}(\text{FOD})_3$ chelates, however, are reported to be considerably more hygroscopic than the $\text{Ln}(\text{DPM})_3$ chelates. The anhydrous FOD complexes absorb one mole of water per each metal atom when left in a moist atmosphere.

In summary, we can tabulate the characteristics of the most commonly used LSRs:

- 1) The lanthanide chelates are Lewis acids with the FOD chelates being more acidic than the DPM chelates.
- 2) The central lanthanide atom can have coordination numbers of six to eight in these LSRs.
- 3) The lanthanide chelates are hygroscopic solids.

*One exception to the greater solubility of the FOD chelates is the fact that $\text{Yb}(\text{DPM})_3$ is more soluble in CCl_4 than $\text{Yb}(\text{FOD})_3$.

- 4) In the $\text{Ln}(\text{DPM})_3 \cdot 2\text{py}$ type crystal structure there is no axial symmetry with respect to the pyridine adducts.
- 5) The $\text{Ln}(\text{DPM})_3$ type chelates have been shown to be structurally non-rigid in solution.

Substrates

Only substrates having one or more Lewis base sites have been found to interact with LSRs. Sanders and Williams¹⁷ reported the following order of interaction of functional group.

amine > hydroxyl > ketone > aldehyde > ether > ester > nitrile

These same authors found that phosphines and nitro groups exhibited weak interactions with LSRs while halides, indoles and olefins were inert to LSRs. Hart and Love¹⁸ have conducted a series of inter- and intramolecular competition experiments to determine the relative coordinating ability of various functional groups. The following order was reported:

ether > thioether > ketone \approx ester

Unsaturation near the ether function decreased the magnitude of the ether-LSR interaction.

Ernst and Mannschreck¹⁹ have attempted to assess some of the factors affecting induced shifts by measuring the shifts induced by $\text{Eu}(\text{DPM})_3$ in a series of para-substituted anilines. The authors reported a linear correlation between the induced shifts and the pK_a values of the amines. N-methyl substitution, although increasing the basicity of the particular amine, was found to cause smaller

observed shifts per mole of LSR. This observation was rationalized by steric effects. Armarego, Batterham and Kershaw²⁰ carried out an extensive study in the shifts induced in 23 π -deficient nitrogen bases by $\text{Eu}(\text{DPM})_3$. The authors found that the pK_a s of these bases could not be used to predict the order of the induced shifts. Again these results were rationalized by means of steric effects.

Many other functional groups have been found to interact with LSRs. Some of these functional groups along with selected references are shown in Table II.

It is clear that the bond formed between the lanthanide metal in the LSR and the functional group in the substrate can be rationalized by a Lewis acid-Lewis base interaction. However, the question still remains whether this system is best treated as a static or dynamic one.

The Dynamic Nature of the LSR-Substrate Association

Taube² rationalized the shift induced in the presence of the paramagnetic salts, by the existence of a rapid exchange between the waters of hydration of the paramagnetic $\text{Co}(\text{II})$ ion and the unbound water molecules. In 1963, Eaton²¹ explained the large shifts observed in the proton spectrum of nickel(II) aminotroponoiminates by the existence of an intramolecular interconversion of a diamagnetic to paramagnetic form of the $\text{Ni}(\text{II})$ compound. Eaton concluded that the shift resonances were the average of the resonances in the diamagnetic $\text{Ni}(\text{II})$ compound and the resonances in the paramagnetic $\text{Ni}(\text{II})$ compound if both the time required for establishing the equilibrium between the two forms and the electronic

TABLE II
SOME FUNCTIONAL GROUPS WHICH HAVE BEEN REPORTED TO INTERACT WITH
LSRs

Functional Group	Reported by
Oximes	Berlin and Rengaraju ²² Wolkowski ²³ Tronchet, <u>et al.</u> ²⁴
Nitrones	Sanders, <u>et al.</u> ²⁵
N-oxides	Johnson, <u>et al.</u> ²⁶ Fletton, <u>et al.</u> ²⁷
Nitrosamines	Fraser and Wigfield ²⁸
Azoxy compounds	Rondeau, <u>et al.</u> ²⁹
Amides	Wolkowski, <u>et al.</u> ³⁰ Lewin ³¹ Isbrandt and Rogers ³² Ward, <u>et al.</u> ³³
Thioamides	Lewin ³¹
Sulphoxides	Andersen and Uebel ³⁴ Fraser and Wigfield ³⁵
Thiocarbamate esters	Bauman ³⁶
Thioamides	Walter, <u>et al.</u> ³⁷
Thioethers	Hart and Love ¹⁸
Diothiolane oxides	Kato and Numata ³⁸
Phosphoryl compounds	Kashman and Awerbouch ³⁹
Phosphorus heterocycles	Yee and Bentrude ^{40,41}
Phosphine oxides	Cuddy, <u>et al.</u> ⁴²

TABLE II CONTINUED

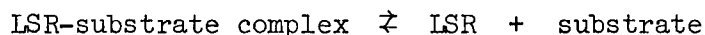
SOME FUNCTIONAL GROUPS WHICH HAVE BEEN REPORTED TO INTERACT WITH
LSRs

Functional Group	Reported by
Alcohols	Rabenstein ⁴³ Smentowski and Stipanovic ⁴⁴ Paasivirta ^{45,46} Paasivirta and Malkonen ⁴⁷
Ketones and aldehydes	Wolkowski ⁴⁸ Kirstiansen and Ledaal ⁴⁹
Ethers	Dale and Kristiansen ⁵⁰ Grotens, Smid and Boer ⁵¹
Ketals	Herz, Rodriguez and Joseph-Nathan ⁵²

relaxation time was shorter than the reciprocal of the magnitude of the observed shift in Hz.

In 1969, Hinckley¹ postulated that the shifts induced by $\text{Eu}(\text{DPM})_3$ in the proton spectra of cholesterol were due to the formation of an oriented complex consisting of the LSR and the cholesterol molecule. In 1972, Evans and Wyatt⁵³ studied the proton spectra of various mixtures of dimethylsulfoxide in CDCl_3 , in the presence of $\text{Eu}(\text{FOD})_3$, at various temperatures from -80°C to room temperature. The spectrum at -80°C showed two resonances. One resonance was assigned to the free dimethylsulfoxide and the other assigned to the dimethylsulfoxide complexed with $\text{Eu}(\text{FOD})_3$. It is clear therefore, that a rapid exchange occurs at room temperature between the substrate molecules in a free state and in the LSR-substrate complex.

In summary, the LSR-substrate interaction can be described in terms of a Lewis acid-Lewis base type complex. The substrate molecules in solution are in a rapid exchange at room temperature.



The equation above serves to illustrate the exchange. Please note no attempt at defining the stoichiometry of the system is being made. This aspect of the description of the LSR-substrate complex will be dealt with in the next section.

CHAPTER IV

AN EVALUATION OF THE VARIOUS DATA TREATMENT TECHNIQUES

IV. AN EVALUATION OF THE VARIOUS DATA TREATMENT TECHNIQUES

A thorough quantitative treatment of the NMR spectra of rapidly exchanging organic charge-transfer complexes can be found in the work of Foster and Fyfe.⁵⁴ If the complexation occurs more rapidly than the NMR time scale, the following expression can be written for the j'th resonance in a given substrate

$$\delta_{\text{obs}}^j - \delta_S^j = \frac{1}{S_0} \sum_{i=1}^N n_i C_i (\delta_{C_i}^j - \delta_S^j) \quad (1)$$

where δ_{obs}^j is the observed chemical shift of the j'th resonance, δ_S^j is the chemical shift of the j'th resonance in the free substrate, S_0 is the molar concentration of substrate, n_i is the number of substrate molecules in the i'th type of complex, C_i is the molar concentration of the i'th type of complex, and $\delta_{C_i}^j$ is the chemical shift of the j'th resonance in the i'th complex.

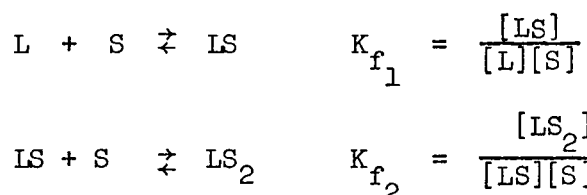
Shapiro and Johnston⁵⁵ have pointed out that a rigorous solution of the concentration dependence of the chemical shift requires the derivation of at least $2N$ parameters, N equilibrium constants for N different complexes and a set of $\delta_{C_i}^j$'s for each complex. In 1969, Derenleau⁵⁶ warned that the concentration of all interacting species must be varied as widely as possible in order to avert disastrous errors in interpreting the time averaged phenomena of these complexes. Since the concentration range used by most researchers is the region

*It should be noted that more than one type of substrate ISR complex can be formed.

where the mole ratio of LSR to substrate is between 0 and 1*, conclusions based on the results obtained over these same concentration ranges might, at first glance, seem suspect. As will be discussed later, conclusions based on observations made on even this restricted concentration range can be demonstrated to be chemically sound.

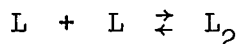
The Stoichiometry of the LSR-Substrate Interaction

Consider the complexation processes occurring in solution



where L is the LSR and S is the substrate concentration, LS, LS₂ are the 1:1 and 2:1 complex respectively, and K_{f₁} and K_{f₂} are the stepwise formation constants.

Shapiro⁵⁵ has determined that Eu(FOD)₃ has a strong tendency for the following self-association process

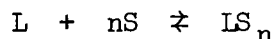


in CCl₄. The equilibrium constant for the above process was determined to be of the order of 3 x 10³. However, Reilley⁵⁷ has determined, by vapor phase osmometry, that both the Pr(DPM)₃ and Eu(DPM)₃ exist as monomers in solution. Furthermore, Reilley concluded that the effect

*The limited solubility of the LSRs coupled with signal to noise considerations make this restricted range experimentally attractive.

of the self-association process of the FOD chelates, in the presence of a large excess of substrate, is small and not even necessarily, reflected in the observed chemical shifts. This same conclusion was reached by Marks⁵⁸ and coworkers in a detailed study of the equilibrium processes in the LSR-substrate system. Therefore, if the concentration range is restricted to the region where the LSR/substrate molar ratio is low, then the self-association process is minimized.

Shapiro⁵⁵ has also reported that Scatchard⁵⁹ plots performed on various lanthanide data, for the process



yielded values of n between 1.3 and 1.7, depending on both the substrate used and the concentration range considered. Roth⁶⁰ and coworkers have used Job's ratio plots to determine the stoichiometry of the LSR-substrate interaction. The authors plotted the incremental change in the observed chemical shift against the $\text{Eu}(\text{DPM})_3$ /substrate mole ratio. The substrates used were *t*-butanol and *t*-butylamine. Maxima were observed, in the respective curves obtained, at a mole ratio of .57. A maximum of .5 is predicted if only the LS type complex is present. If the LS_2 complex were the predominant species, then a maximum would be observed at a mole ratio of .67. Neither Roth's nor Shapiro's results provide a general answer to the stoichiometry of the LSR-substrate complex.

Two problems arise at this point. The first problem is to decide whether a completely rigorous treatment of the concentration

problem is necessary*. The second problem is to find a readily workable[‡] method of data treatment which is consistent with the experimental behavior of the shift, observed in the experimental concentration range.

Experimental Variation of the Induced Shift with LSR/Substrate Concentration

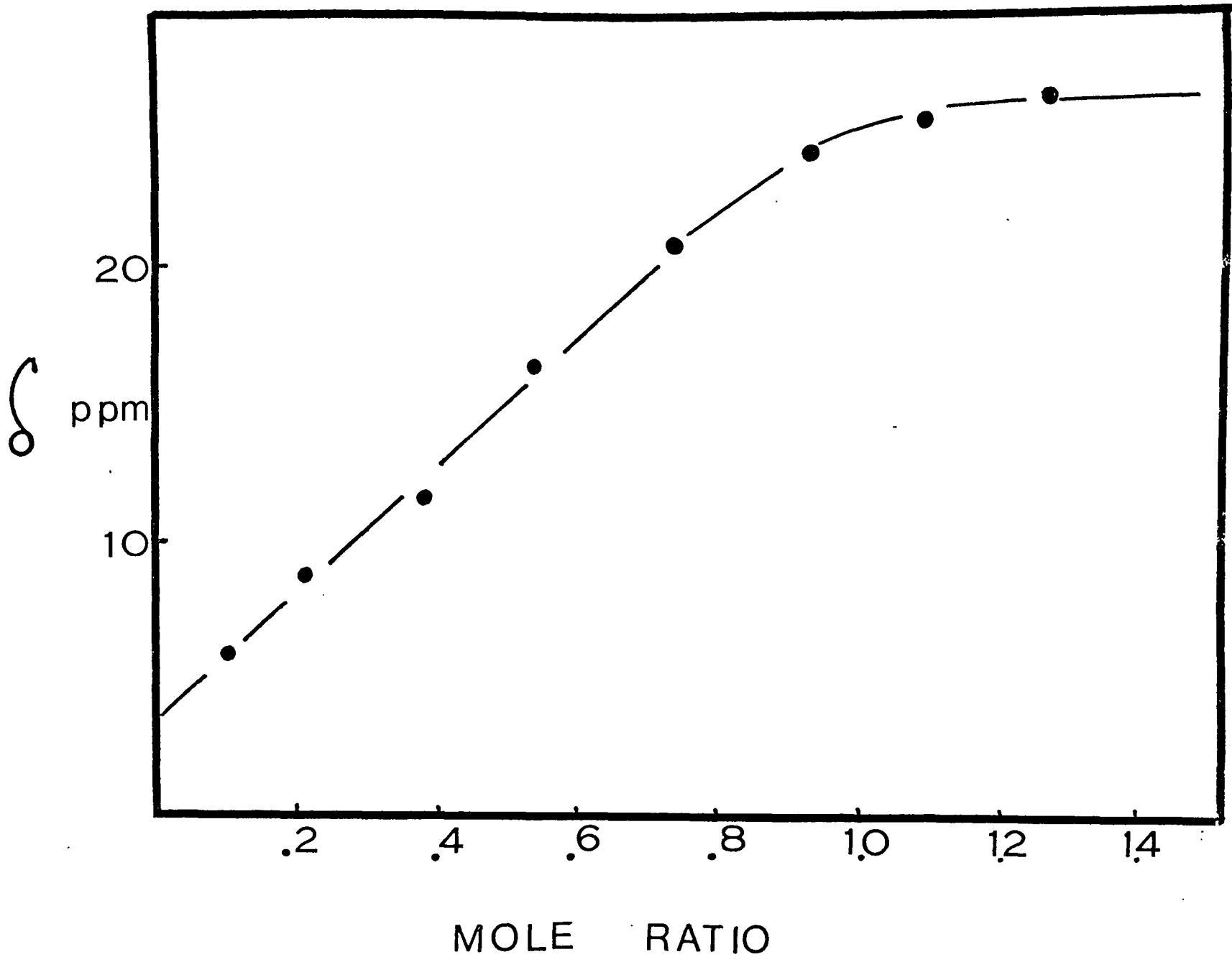
In 1970, Demarco and Wenkert⁶¹ reported that, over the $\text{Eu}(\text{DPM})_3$ -substrate mole ratio range between 0 and .7, the observed proton lanthanide induced shift was a linear function of the $\text{Eu}(\text{DPM})_3$ /substrate mole ratio. The substrates used were 4-t-butylcyclohexanols. Small deviations from linearity were observed at low mole ratios. Rondeau and Sievers⁶² showed that a plot of δ_{obs} against the LSR/substrate mole ratio was linear over the 0 to .7 mole ratio range. These authors also noted that the plot levelled off at a mole ratio of about 1. The LSR used in these studies was $\text{Eu}(\text{FOD})_3$.

Figure 2 shows the typical variation of the observed shift of a given resonance with LSR/substrate mole ratio. Note again that any method of data treatment must use a model consistent with the experimental behavior of the observed shift.

*In this context, necessary should be defined as necessary to be consistent with the experimental behavior.

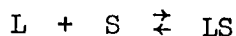
[‡]If the method of data workup requires orders of magnitude more time than the actual shift experiment, then it may be of little use to the chemist who seeks to use shift parameters in structural studies.

FIGURE 2: VARIATION OF THE OBSERVED SHIFT FOR THE H₂ RESONANCE
OF BORNEOL WITH THE MOLE RATIO OF Eu(DPM)₃/BORNEOL



Algebraic Formulation of the Various LIS Data Refinement Methods

Consider the formation of a LS type complex only. As before



$$K_f = \frac{[LS]}{[S][L]} \quad (2)$$

From the mass law, it follows that

$$S_o = [S] + [LS] \quad (3)$$

where S_o is the molar concentration of substrate,

and

$$L_o = [L] + [LS] \quad (4)$$

where L_o is the molar concentration of LSR.

From equation (1), if only a LS type complex is present, then for a given resonance

$$\delta_{obs} - \delta_s = \frac{[LS]}{S_o} (\delta_c - \delta_s). \quad (5)$$

Substituting $[LS] = L_o - [L]$ from (4), into (5) yields

$$(\delta_{obs} - \delta_s) = \frac{(L_o - [L])}{S_o} (\delta_c - \delta_s) \quad (6)$$

Defining $\Delta_m = \delta_{obs} - \delta_s$ and $\delta_c = \delta_c - \delta_s$ in equation (6) gives

$$\Delta_m = \frac{(L_o - [L])}{S_o} \Delta_c \quad (7)$$

As has been noted by Kelsey⁶³, equation (7) can be rearranged to yield

$$\Delta_m = \left(1 - \frac{[L]}{L_o}\right) \left(\frac{L_o}{S_o}\right) \Delta_c. \quad (8)$$

Note, Δ_m is now a function of $\frac{L_o}{S_o}$.

Consider the range where $\frac{[L]}{L_o}$ is small, that is, where $S_o \gg L_o$. In this region, $(1 - \frac{[L]}{L_o}) \approx 1$ and Δ_m is a linear function of $\frac{L_o}{S_o}$ with slope Δ_c . When $\frac{[L]}{L_o}$ is large, that is, at high $\frac{L_o}{S_o}$ mole ratios, the Δ_m would be zero.

These predictions are consistent with the shape of the experimental curve shown in Figure 2.

Demarco⁶¹ Method

Equation (8) can be rewritten as follows:

$$\delta_{obs} - \delta_s = \left(1 - \frac{[L]}{L_o}\right) \left(\frac{L_o}{S_o}\right) (\delta_c - \delta_s)$$

If we confine our considerations to the range where $S_o \gg L_o$, then

$$\delta_{obs} = \frac{L_o}{S_o} (\delta_c - \delta_s) + \delta_s$$

The quantity $(\delta_c - \delta_s)$ can be determined by either measuring the slope of the plot of δ_{obs} against L_o/S_o or by an extrapolation procedure. In 1970, Demarco defined a shift parameter Δ_{Eu} in the following way.

$$\Delta_{Eu} = \delta_{CDCl_3} - \delta_{Eu(DPM)_3}^{n=1}$$

where δ_{CDCl_3} is the observed shift in $CDCl_3$ with no $Eu(DPM)_3$ present and $\delta_{Eu(DPM)_3}^{n=1}$ is the extrapolated shift at a mole ratio of $Eu(DPM)_3$ /substrate of 1.0.

Willcott⁶⁴ and coworkers have used the slopes (Δv_i) of the straight lines, obtained by plotting the position of a given resonance signal (v_i) against the $Eu(DPM)_3$ /substrate mole ratio, to identify the

stereochemistry of the methoxy function in 7-methoxybicyclo[4.3.1]-
deca-1,3,8-triene.

A Rigorous Method

Going back to equation (1)

$$K = \frac{[LS]}{[L][S]},$$

substituting (3) and (4) into (1)

$$K = \frac{[LS]}{(L_o - [LS])(S_o - [LS])}$$

and solving for [LS] yields

$$[LS] = \frac{(S_o + L_o + \frac{1}{K}) \pm [(S_o + L_o + \frac{1}{K})^2 - 4S_o L_o]^{1/2}}{2}. \quad (9)$$

Substituting (9) into (5) gives

$$(\delta_{\text{obs}} - \delta_s) = \frac{\left[(S_o + L_o + \frac{1}{K}) \pm [(S_o + L_o + \frac{1}{K})^2 - 4S_o L_o]^{1/2} \right] (\delta_c - \delta_s)}{2S_o} \quad (10)$$

Defining Δ_m and Δ_c as before yields

$$\Delta_m = \frac{\left[(S_o + L_o + \frac{1}{K}) \pm [(S_o + L_o + \frac{1}{K})^2 - 4S_o L_o]^{1/2} \right] \Delta_c}{2S_o} \quad (11)$$

Digital solution of equation (11), using shift data, yields appropriate values of Δ_c and K_f .

Willcott-Herndon-Lenkinski Method

Consider equation (3),

$$S_o = [S] + [LS] \quad (3)$$

If the measurements are limited to the region where $S_o \gg L_o$, say mole ratios of around .1, then

$$S_o \approx [S] \quad (12)$$

Substituting into (1) and rearranging yields

$$[LS] = \frac{K_o^S L_o}{K S_o + 1} \quad (13)$$

Substituting (13) into (5) and rearranging gives

$$\frac{\Delta_m}{L_o} = -K \Delta_m \left(\frac{S_o}{L_o} \right) + K \Delta_c \quad (14)$$

Plots of $\frac{\Delta_m}{L_o}$ against $\Delta_m \left(\frac{L_o}{S_o} \right)$ should show slopes of $-K$ and ordinate intercepts of Δ_c .

Kelsey Method

Rearranging (13) in a slightly different form yields

$$\frac{1}{\Delta_m} = \frac{1}{\Delta_c} \left(\frac{S_o}{L_o} \right) + \frac{1}{\Delta_c L_o K} \quad (15)$$

This expression has been used by Kelsey⁶³ and by Hall and coworkers⁶⁵ to calculate K_s and Δ_c .

ApSimon Method

ApSimon and Bierbeck⁶⁶ have reported a method for determining a set of internally scaled shift parameters which minimizes the errors in L_o and S_o concentration measurements. The simplicity of this method is attractive. The authors plot the shift of a given resonance (ν_i) against the sum of all the observed shifts ($\sum_{i=1}^N \nu_i$) for each $\frac{L_o}{S_o}$ ratio. The actual $\frac{L_o}{S_o}$ value does not need to be determined. The slopes of the straight lines obtained from the above plots generate a set of internally scaled shift parameters for the substrate being investigated. The fact that no absolute magnitudes of shift parameters can be determined by the ApSimon method might seem disadvantageous. However, as will be shown later, in most applications of LSRs to organic structure determinations, the relative magnitudes of shift parameters are sufficient.

Summary of the Various Data Work-Up Schemes

There are five methods of treating the data from lanthanide shift experiments. Briefly, the methods are:

- 1) the simple plotting of δ_{obs} against L_o/S_o to determine shift parameters by extrapolation procedure and slope measurement,
- 2) the plotting of Δ_m/L_o against $\Delta_m(\frac{S_o}{L_o})$ in equation (14) to give the slopes of $-K$ and ordinate intercepts of Δ_c ,
- 3) the digital rigorous solution of equation (11) to yield Δ_c and K ,
- 4) the plotting of $\frac{1}{\Delta_m}$ against $(\frac{S_o}{L_o})$ to give slopes of $\frac{1}{\Delta_c}$ and intercepts of $\frac{1}{\Delta_o L_o K}$.

and

5) the ApSimon method of plotting ν_i against $\sum_{c=1}^N \nu_i$ to yield scaled shift parameters.

In order to compare the results of these five methods of data work-up, we decided to compute the LIS indices for some simple molecules using the same set of experimental spectra as a starting point. We felt that a comparison of the LIS indices generated by the five different methods would indicate which of the five methods was the most convenient one to use in further experiments.

Experimental Procedure

All solvents and the liquid substrates were dried over molecular sieves for a period of three days before use. The $\text{Eu}(\text{DPM})_3$ and $\text{Pr}(\text{DPM})_3$ were synthesized following the procedure of Rondeau and Sievers.⁹ The crude $\text{Eu}(\text{DPM})_3$ and $\text{Pr}(\text{DPM})_3$ chelates were recrystallized twice from hexane. The recrystallized chelates were dried over P_2O_5 in a Aberhalden drying pistol, at 100°C , under vacuum, overnight before use.

(1) Tetrahydrofuran (THF) - $\text{Eu}(\text{DPM})_3$ in CCl_4

A 100 MHz ^1H spectrum of 0.5 ml of a CCl_4 solution containing 5.7 mg $\text{Eu}(\text{DPM})_3$ (0.0142M) and 5.24 mg THF (0.146M) was taken on a Varian HA100 instrument. Then spectra were obtained as 2 to 5 μl aliquots of THF were added. This sequential addition was halted when a total of 45 μl (1.166M) THF was present. In each spectrum, an $\alpha\text{-CH}_2$ and $\beta\text{-CH}_2$ resonance position was measured to within ± 1 Hz relative to TMS as internal standard. The data obtained from the experiment was subjected to the five different methods of data work-up outlined on page 26. In all cases except method III, a linear least squares refinement was performed on the appropriate values to yield shift parameters. In method III, equation (11), on page 24 was solved digitally by an interactive computer scheme. The convergence of the data fit was assayed by $\sum_i (\Delta_{m_i \text{ calc}} - \Delta_{m_i \text{ obs}})^2$.

The least squares program used in the other data work-up schemes was a standard single precision linear regression analysis. The algorithm was an adaptation of a library routine available at the University of Houston Computer Center. The adaptation was carried out by Robin Isaacs.

(2) Pyridine-Eu(DPM)₃ in CCl₄

A 100 MHz ¹H spectrum of a 0.5 ml solution of CCl₄ containing 8.93 mg pyridine (0.226M) and 9.35 mg Eu(DPM)₃ (0.0227M) was obtained. Then spectra were obtained as 2 to 5 μl aliquots of pyridine were added. The sequential addition of pyridine was halted when a total of 30 μl of pyridine had been added. The various proton resonances were measured in each spectrum relative to TMS internal reference. As before, the raw data obtained from this experiment was refined using all five methods outlined on page 26. The least squares refinement was carried out as before in all cases except III, where the same algorithm was performed as outlined in the previous sections.

(3) Pyridine - Pr(DPM)₃

A 100 Mz ¹H spectrum of 0.5 ml solution of CCl₄ containing 8.93 mg pyridine (0.226M) and 14.98 mg Pr(DPM)₃ (.0441M) was obtained. Then spectra were taken as 2 to 5 μl aliquots of pyridine were added. This sequential addition was halted when a total of 40 μl of pyridine had been added. The three different proton resonances were measured to within ±.1 Hz using TMS as internal standard. As before, the raw data obtained was refined using the five methods outlined on page 26.

A Comparison of the Results of the Five Methods of Data Treatment
in Lanthanide Induced Shift Experiments

A partial summary of the five different methods of data treatment is shown in Table I. In column IV of Table III, a summary of the experimental conditions for each method is presented. Note that methods I, III, and V are experimentally the most convenient. Consider method II. Equation (14) on page 25,

$$\frac{\Delta_m}{L_o} = -K \frac{\Delta_m}{L_o} S_o + K \Delta_c \quad (14)$$

is the equation upon which method II is based. If L_o is varied, while S_o is kept constant, the equation is of the form

$$\frac{\Delta_m}{L_o} = \text{constant} \left(\frac{\Delta_m}{L_o} \right) + \text{constant}$$

which yields no physically significant result upon solution. Therefore equation (14) only applies to data obtained from experiments where L_o has been kept constant and S_o varied.

Consider equation (15) on page 25,

$$\frac{1}{\Delta_m} = \frac{1}{\Delta_c} \frac{S_o}{L_o} + \frac{1}{\Delta_c L_o K} ,$$

upon which method IV is based. If L_o is varied while S_o is kept constant, then the equation can be rewritten as

$$\frac{1}{\Delta_m} = \left(\frac{S_o}{\Delta_c} + \frac{1}{K \Delta_c} \right) \frac{1}{L_o} \quad (15)$$

TABLE III
A SUMMARY OF THE VARIOUS TECHNIQUES OF DATA TREATMENT IN LANTHANIDE
INDUCED SHIFT (LIS) EXPERIMENTS

Method	Developed or reported by	Variable necessary for computation	Experimental conditions	average computation time(g)
I	M. R. Willcott, <u>et al.</u> ⁶⁴ P. V. Demarco, <u>et al.</u> ⁶¹	ν_i (c), L_o (d)/ S_o (e)	Can vary S_o and L_o . Measure ν_i for each spectrum.	1 hour / .1 sec.
II	M. R. Willcott, R. E. Lenkinski and W. C. Herndon ^(a)	Δ_{m_i} (f), $\Delta_m \frac{S_o}{L_o}$	Must keep L_o constant, can vary S_o . Measure Δ_{m_i} for each spectrum.	1 hour / .1 sec.
III	M. R. Willcott and R. E. Lenkinski ^(a)	S_o , L_o , Δ_m	Can vary S_o and L_o . Measure Δ_{m_i} for each spectrum.	1 hour / 2 sec.
IV	A. G. Marshall, <u>et al.</u> ⁶⁵ D. R. Kelzey ⁶³	$\frac{1}{\Delta_m}$, S_o	Must keep L_o constant, vary S_o and measure Δ_{m_i} for each spectrum.	1 hour / .1 sec.
V	J. W. ApSimon and H. Beierbeck ⁶⁶	ν_i , $\sum \nu_i$	Can vary S_o and L_o . Measure ν_i for each spectrum.	1/2 hour / .1 sec.

(a) Unpublished results.

(b) Unpublished results.

(c) ν_i is the position of the i'th resonance in each altered spectrum.

(d) L_o is the formal concentration of LSR.

(e) S_o is the formal concentration of substrate.

(f) Δ_m is the incremental change in chemical shift for the i'th resonance.

(g) X/Y X is the number of man hours, Y is the amount of Univac 1108 C.P.U. time.

This equation is of the form

$$y = mx$$

$$\text{where } m = \left(\frac{S_o}{\Delta_c} + \frac{1}{K\Delta_c} \right)$$

$$\text{and } y = \frac{1}{\Delta_m}, \quad x = \frac{1}{L_o}$$

The slope, m , however, contains two unknown quantities, Δ_c and K . No physically significant information can be obtained from the slope. Therefore equation (15) only applies to data obtained from experiments where L_o has been kept constant and S_o varied. In some cases, these experimental restrictions become critical. For example, if only a small amount of substrate is available (10-20 mg), then S_o cannot be varied appreciably and one of methods I, III or V must be used.

The five different pairs of shift indices for the THF-Eu(DPM)₃ system are shown in Table IV. It is clear that, although the absolute magnitude of a shift index differs considerably from method to method, the ratio of the shift parameters within a given method are virtually indistinguishable. The average value of the α/β ratio is also shown in Table IV along with a standard deviation for this average. In the case of THF, at least, the internal α/β shift ratios generated by the five different methods fall within a range of $\pm 2\%$ of one another.

The shift indices for the pyridine-Eu(DPM)₃ experiment generated by the five different computational schemes are also shown in Table IV. Again, although the absolute magnitude of the shift indices differ as much as 15 ppm, as in the case of the α proton of pyridine, the rescaled

TABLE IV
A COMPARISON OF THE SHIFT INDEXES COMPUTED BY FIVE DIFFERENT METHODS ON
THF-Eu(DPM)₃ AND PYRIDINE Eu(DPM)₃ DATA

Method ^(a)	THF			Pyridine			Rescaled Pyridine ^(b)		
	α	β	α/β	α	β	γ	α'	β'	γ'
I	26.8 ±.5	11.9 ±.1	2.25 ±.06	35.9 ±.5	12.3 ±.2	11.2 ±.1	.604 ±.008	.207 ±.004	.189 ±.002
II	31.0 ±.5	13.7 ±.5	2.26 ±.09	42.2 ±1.0	14.0 ±.5	12.8 ±.3	.612 ±.01	.203 ±.005	.486 ±.003
III	31.0 ±1	14.0 ±.3	2.22 ±.07	43.3 ±1	14.2 ±.5	13.2 ±.3	.612 ±.01	.201 ±.005	.187 ±.003
IV	30 ±.5	13.8 ±.4	2.20 ±.06	53.2 ±1	17.3 ±.6	16.6 ±.4	.611 ±.01	.199 ±.005	.191 ±.003
V	.690 ±.005	.310 ±.003	2.25 ±.04	.616 ±.01	.206 ±.005	.195 ±.003	.616 ±.01	.206 ±.005	.195 ±.003
Average			2.23				.611	.203	.189
Standard Deviation			.03				.008	.003	.004

(a) See Table III and page 26 for identification of each method.

(b) Rescaled values were obtained by taking $\alpha' = \frac{\alpha}{\alpha+\beta+\gamma}$, $\beta' = \frac{\beta}{\alpha+\beta+\gamma}$, $\gamma' = \frac{\gamma}{\alpha+\beta+\gamma}$

TABLE V
A COMPARISON OF THE SHIFT INDEXES COMPUTED BY FIVE DIFFERENT METHODS
ON PYRIDINE-Pr(DPM)₃ DATA

Method ^(a)	Pyridine			Rescaled Pyridine Indexes ^(b)		
	α	β	γ	α'	β'	γ'
I	57.5 ±1	20.0 ±1	16.4 ±.8	.616 ±.01	.213 ±.005	.174 ±.003
II	74.2 ± 2	27.3±.8	21.1±.6	.602±.006	.222±.004	.175±.005
III	77. ± 2	28.4±1	22. ±1	.605±.007	.223±.006	.172±.006
IV	79.2 ± 2	28.9±1	23.4±1	.603±.008	.220±.008	.177±.008
V	.616 ± .006	.211±.004	.174±.003	.616±.006	.211±.004	.174±.003
Average				.608	.215	.174
Standard Deviation				.007	.006	.002

(a) Methods are identified in Table III and on page 26.

(b) The indexes were rescaled as in Table IV $\alpha' = \frac{\alpha}{\alpha+\beta+\gamma}$, etc.

shift parameters are virtually indistinguishable within $\pm 2\%$ of another. The average value for each rescaled shift index is also given in Table IV along with a standard deviation for each average. It would seem that, as long as relative shift parameters are being considered instead of absolute shift parameters, all five methods of data treatment give the same result, within $\pm 2\%$, in the pyridine-Eu(DPM)₃ system.

The results of the pyridine-Pr(DPM)₃ experiment are shown in Table V. The absolute shift parameters have been rescaled again to facilitate a comparison of the results of the computational method. Again, the absolute magnitude of the shift parameters differ as much as 20 ppm, in the α -proton shift index, from method to method. However, the rescaled indices remain virtually the same from method to method. The average value for each rescaled shift index is shown in Table V, along with a standard deviation for each average. Clearly the five methods generate relative shift parameters which are indistinguishable within experimental error. This same conclusion has been reached in a study of adamantylamines, with Eu(FOD)₃ and Yb(FOD) performed by Goerland⁶⁷ in our laboratories.

If we compare the average rescaled values for the Pr(DPM)₃ and Eu(DPM)₃ pyridine data we find

	α	β	γ
Pr(DPM) ₃	.611	.203	.181
Eu(DPM) ₃	.608	.218	.174

These results are not identical. The differences between the two sets of results fall outside of the range of experimental error. Since the values are scaled shift parameters, this discrepancy leads to the conclusion that the effect causing the shift in both cases is not identical. This point will be discussed more fully in the next chapter.

Since the results of the five computational schemes are the same, the next consideration made will be on the time required to perform each computation. Returning to Table III, the average time required to perform each computation is shown in column V. Note that the shortest computational scheme, in terms of man hours, is method V, the Apsimon⁶⁶ method. The longest computational scheme, in terms of computer time is method III. Also note, that the other four methods consume about equal amounts of computer time. Therefore method III is not an attractive method, since it involves both more computer time and more man hours of computation than any other.

As has been pointed out, methods II and IV suffer from the fact that L_0 must be kept constant. Therefore methods I and V seem to offer clear cut advantages over the other three methods. The number of experimentally measurable quantities necessary for each of these five methods is compared in column III of Table III. All methods, except method V, involve three measured quantities. These are a measured set of resonance positions for each altered spectrum, the concentration of substrate present in each case, and the concentration of LSR present in each case. Method V involves only the measurement of a set of resonance positions for each altered spectrum. This elimination of two measured

quantities, in method V, results in a reduction in the source of errors made in measurement. It is clear that based upon considerations of time, ease of measurement, and experimental applicability, the ApSimon⁶⁶ method has many advantages over the other four schemes. Note that this statement is based on the assumption that only relative, not absolute, shift indexes are required for obtaining further desired results.

CHAPTER V
CONSTRUCTION OF THE MODEL FOR THE LSR-SUBSTRATE
INTERACTION

V. CONSTRUCTION OF THE MODEL FOR THE LSR-SUBSTRATE
INTERACTION

A. Theoretical Considerations

A simplified Hamiltonian for a nucleus in the presence of the paramagnetic lanthanide metal is given by²

$$H_N = -\gamma \hbar \vec{I} \cdot \vec{H}_0 + \vec{I} \cdot \vec{A} \cdot \vec{S} + \sum_i \beta \alpha \vec{I} \cdot \vec{g} \cdot \vec{S} (1 - 3 \cos^2 \theta_i / r_i^3) \quad (1)$$

where the first term, $\gamma \hbar \vec{I} \cdot \vec{H}_0$ represents the Zeeman energy of the nucleus in a diamagnetic medium.

The second term represents the hyperfine interaction between the rare earth atom and the nucleus, resulting from the weak admixture of the wavefunctions of the rare earth with the wavefunctions of the particular atom in question. The third term represents the magnetic dipole interaction between the nuclear magnetic moment and the electronic moment of the rare earth ion. The second term is referred to as the contact term while the third term is referred to as the dipolar or pseudocontact term. The observed shift induced by the presence of the lanthanide can be written as follows.⁶⁸

$$\delta_{\text{obs}} = \delta_s + \delta_{\text{contact}} + \delta_{\text{pseudocontact}} \quad (2)$$

Where δ_s is the observed shift with no LSR present, δ_{contact} is the shift caused by the contact interaction and $\delta_{\text{pseudocontact}}$ is the shift caused by the pseudocontact interaction.

δ_{contact}

The contact shift for the lanthanides has been written in the following form by Reuben⁶⁹ and Taube².

$$\delta_c = \frac{-2\pi\beta\nu AJ(J+1)g_L(g_L-1)}{3KT\gamma} \quad (3)$$

where ν and γ are the nuclear Larmor frequency and magnetogyric ratio, β is the Bohr magneton, J is the resultant electronic spin angular momentum (\hbar units), g_L is the Lande g -factor and A is the scalar coupling constant in Hz.

Shulman^{70,71} has related the coupling constant to the fractional spin occupancy by

$$A = \frac{f_s A_s}{2S} \quad (4)$$

where A_s is the isotropic coupling constant due to one unpaired electron in an s orbital and $2S$ is the number of unpaired electrons on the lanthanide and f_s is the fractional spin occupancy.

For nuclei in the same molecule the contact shift is

$$\delta_c \sim \frac{f_s A_s}{\gamma} \quad (5)$$

 $\delta_{\text{pseudocontact}}$

McConnell and Robertson⁶⁸ have derived an expression for the pseudocontact shift for transition metals. This derivation makes the assumption that the magnetic susceptibility tensor is axially symmetric.

$$\delta_p = \frac{-\nu\beta^2(J)(J+1)}{3KTr^3} (3\cos^2\theta-1)(g_{11} + g_1)(g_{11}-g_1) \quad (6)$$

where r is the vector distance from the given nucleus to the magnetic dipole and θ is the angle formed between the given nucleus and the principal or effective⁷² principal magnetic axis. Note this expression for the dipolar or pseudocontact expression is the point dipole field perturbation expression. A graphical description of the terms (r, θ, Ω) is shown in Figure 3. Note again that this expression, equation (6), is based on the assumption that the complex in question has an axially symmetric magnetic susceptibility tensor. That is, $\chi_{11} = \chi_z$, $\chi_1 = \chi_x = \chi_y$ or, in terms of anisotropy parameters

$$g_{11} = g_z, g_1 = g_x = g_y$$

LaMar, Horrocks and Allen⁷³ have derived the expression for the pseudocontact term in the case where there is an asymmetric anisotropy or magnetic susceptibility tensor

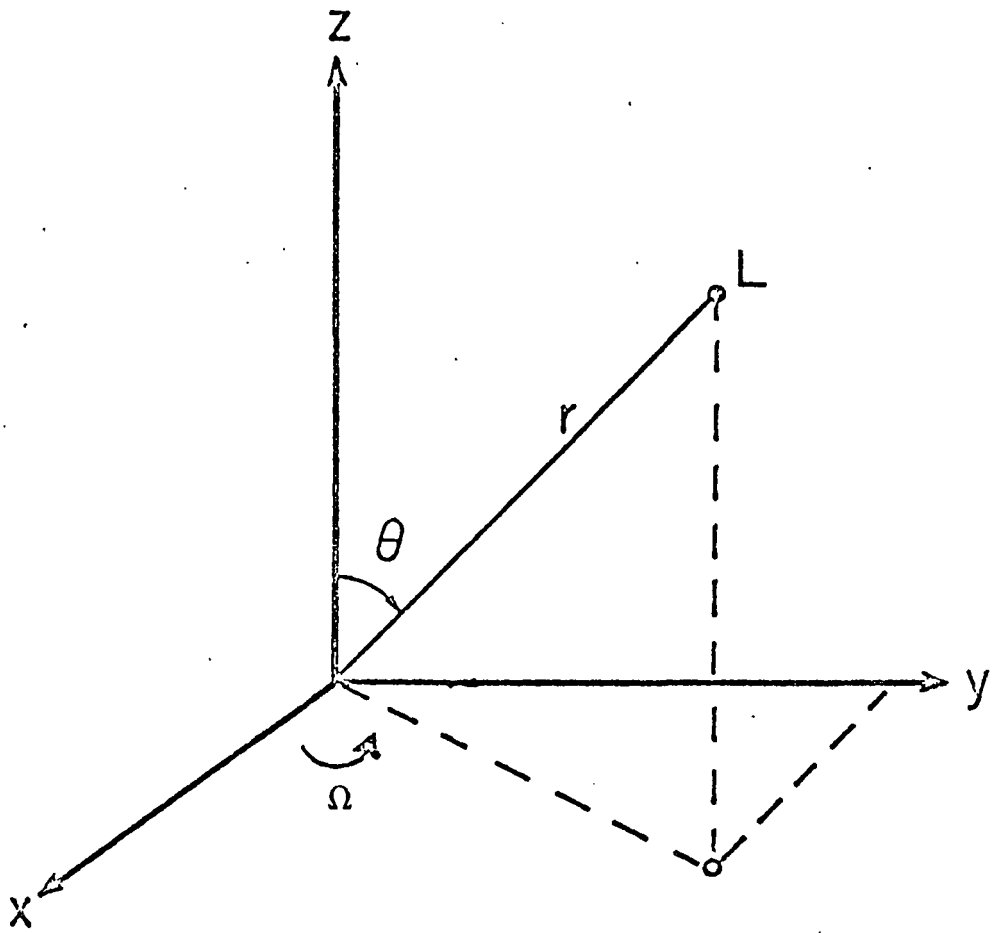
$$\delta_p = \frac{-\nu\beta^2 J(J+1)}{9KT} \left[\left(\frac{g_z^2}{2} - \frac{g_x^2}{2} - \frac{g_y^2}{2} \right) \left(\frac{3\cos^2\theta-1}{r^3} \right) - \frac{3}{2} (g_x^2 - g_y^2) \left(\frac{\sin^2\theta \cos 2\Omega}{r^3} \right) \right] \quad (7)$$

where r and θ are defined as in (6) and Ω is shown in Figure 3.

In summary, the problems involved in constructing a model for the LSR-substrate interaction are

- I. Should the observed shifts be factored into contact and pseudocontact contributions?
- II. Is the use of the McConnell-Robertson relationship for axially symmetric ions appropriate?
- III. What orientation of the principal magnetic axis should be used for the computer simulation of the LIS experiment?

FIGURE 3: A GRAPHICAL DEFINITION OF r , θ AND Ω , THE VARIABLES DESCRIBED IN THE MCCONNELL-ROBERTSON EXPRESSION



Justification of the Pseudocontact Model for ^1H LIS Data

Referring to equation (5),

$$\delta_c \sim \frac{f_s A_s}{\gamma},$$

as assessment of the relative contact shifts for various nuclei having the same spin occupancy can be made. This assessment, carried out by Goodman and Raynor⁷⁴, is shown in Table VI. From column III, it is clear that the ^1H nucleus is the least susceptible to contact interactions. All other nuclei are at least one order of magnitude more susceptible to contact interactions than the ^1H nucleus. This calculation was carried out on the assumption that the sets of nuclei have the same spin occupancy. In the LSR-substrate complexes, the heteroatoms are the ones involved in the bonding with the LSRs. The ^1H nuclei are generally removed from the bonding interaction. Therefore, the assumption of equal spin occupancy generates an upper limit on the magnitude of the relative contact interaction in proton LIS experiments. For example, Reuben and Fiat⁶⁹ have reported a 474 ppm shift in the ^{17}O resonance of water in the presence of $\text{Gd}(\text{ClO}_4)_3$, whereas the corresponding ^1H shift was only 3 ppm.

The literature abounds⁷⁵⁻⁷⁹ with the pseudocontact description of proton shifts induced by various shift reagents. Except in a very few cases, such as some pyridine-N-oxides in the presence of $\text{Eu}(\text{DPM})_3$ ²⁶ and some substituted pyridines in the presence of Praeseodymium and Neodymium salts⁸⁰; the pseudocontact model seems satisfactory. Reuben⁸¹ has estimated the relative importance of the pseudocontact

TABLE VI
RELATIVE CONTACT SHIFTS FOR NUCLEI IN THE SAME MOLECULE
AND OF THE SAME FRACTIONAL SPIN OCCUPANCY

Nucleus	A_s , gauss ^(a)	$\frac{\Delta_c^N}{\Delta_c^{1H}}$
1H	508	[1.00]
^{13}C	1119	8.76
^{14}N	557	15.18
^{17}O	1659	24.06
^{19}F	17160	35.90
^{31}P	3676	17.84

(a) From ref. 74.

shift along the lanthanide series by taking the ratio

$$(\chi_z - \frac{1}{2}\chi_x - \frac{1}{2}\chi_y) / [g_L(g_L - 1)J(J+1)]$$

as a measure of $\frac{\delta_c}{\delta_p}$ where χ_z is the magnetic susceptibility along a defined z direction. Using anisotropy data from Horrocks and Sipe⁸² in the numerator leads to

Ln ³⁺	Pr	Nd	Eu	Tb	Dy	Ho	Er	Yb
δ_p/δ_c	1000	277	160	503	870	447	238	1340

Clearly Eu³⁺ should be the lanthanide most likely to induce contact shifts while Yb should be the least likely to induce contact shifts. Stated in another way, the shifts induced by Yb should fit the pseudocontact description best.

The results of the pyridine LIS experiments formed with both Pr(DPM)₃ and Eu(DPM)₃ from Table IV and V are tabulated below.

	α'	β'	γ'
Eu(DPM) ₃	.608	.218	.174
Pr(DPM) ₃	.611	.203	.181

Earlier reference was made to the fact that these two sets of rescaled shift indices were not identical. This discrepancy in the shift indices can be explained by the presence of contact shifts in either one, or both, of the two compounds. From the previous estimates of δ_p/δ_c , it is more likely that the Eu(DPM)₃ induced shifts contain some contact contribution. As has been concluded earlier, the ¹H nucleus is expected to be the least susceptible to contact interactions.

In other nuclei such as ^{13}C , ^{17}O and ^{19}F , the contact shifts should be much larger.

In summary, it would seem that the pseudocontact model for lanthanide induced shifts in ^1H NMR is applicable to most substrate systems. However, when using shift reagents, one must be conscious of the fact that europium can, in some cases, introduce large contact shifts in even the proton spectra of these substrates. The lack of line broadening, when using europium, makes europium LSRs attractive experimentally.

The Question of Axial Symmetry

The question of axial symmetry, in lanthanide shift reagent-substrate complexes, has been the topic of much heated debate in the literature. There are, in our view, several justifications for assuming effective axial symmetry in the LSR-substrate complexes, although there is no evidence of axial symmetry in the crystal structures of some of the LSR-substrate complexes.

The structures of these complexes determined in their crystalline form are essentially static structures, while the LSR-substrate system is a dynamic system in solution. Horrocks¹¹ has pointed out that the structures determined by X-ray crystallography are not necessarily maintained in solution. It is instructive to consider, at this point, the various dynamic processes that can occur in these kinds of systems, in solution.

The LSR-substrate systems may undergo;

- (1) fluctuational isomerization (intramolecular reorganization),
- (2) intermolecular ligand exchange

or

- (3) the rapid intermolecular substrate exchange described in Chapter III.

At room temperature, only one set of shifted substrate resonances as well as a single broad ligand resonance are observed. If we assume that the observed ligand resonance is the time average, at room temperature, of various non-equivalent resonances and if the rate of the intermolecular reorganization of the various non-equivalent ligand molecules is much faster than the intermolecular substrate exchange process, then the two sets of substrate resonances* would appear at a higher temperature, in the low temperature NMR experiment, than the resonances due to the magnetic non-equivalence of the t-butyl group in the ligand. When the variable temperature NMR experiments are performed,⁵³ two sets of substrate resonances are observed at around -80°C in the dimethylsulfoxide $\text{Eu}(\text{FOD})_3$ system. At this time, no one has been able to observe the various resonances due to the magnetic non-equivalence of the ligand t-butyl groups. Therefore, it is safe to conclude that the intramolecular reorganization of the LSR, in solution, at room temperature,

*The resonances due to the free substrate molecule as well as the resonances of the LSR-substrate complex.

occurs much faster than the intermolecular substrate exchange. The presence of this intramolecular reorganization seems to cause effective axial symmetry in the LSR-substrate systems.

Another consideration that must be made involves the maximum number of determinable parameters one can obtain in a LIS experiment. Clearly, in order for the LSR-substrate system to be well-defined, the number of observations available* must exceed the number of determinable parameters. In a previous section, the applicability of the pseudocontact model to LIS data for ^1H nuclei was discussed. In almost all cases, the ^1H data was shown to be pseudocontact in origin. Now the question becomes: Is the axially symmetric pseudocontact model or is the axially-asymmetric pseudocontact model appropriate for the replication of ^1H LIS data?

Equation (6) can be rewritten in the following form

$$\delta_p = K_1 \left(\frac{3\cos^2\theta - 1}{r^3} \right) \quad (8)$$

$$\text{where } K_1 = \frac{\nu K J(J+1)}{3KT} (g_{11} + g_1)(g_{11} - g_1)$$

K_1 should be constant if we consider only one set of substrate resonances. If the shift indices, discussed in Chapter IV, are completely pseudocontact in origin for H^1 data, then there are at least four[†] parameters, which must be determined in order to make equation (8) well-defined.

*The number of observations is the number of measured LIS indices in the molecule.

†The parameters are the three positional parameters of the lanthanide atom (r , θ , Ω) and K_1 .

If equation (7) is rewritten in the following form,

$$\delta_p = K_1 \left(\frac{3\cos^2\theta - 1}{r^3} \right) + K_2 \left(\frac{\sin^2\theta \cos 2\Omega}{r^3} \right), \quad (9)$$

there is one additional parameter K_2 which must be determined. In some cases, there may not be a sufficient number of ^1H LIS observations available to permit the use of the axially-asymmetric model, equation (9). Clearly equation (8), the equation for the effectively axially-symmetric model, is more economical in terms of the number of observations one must make.

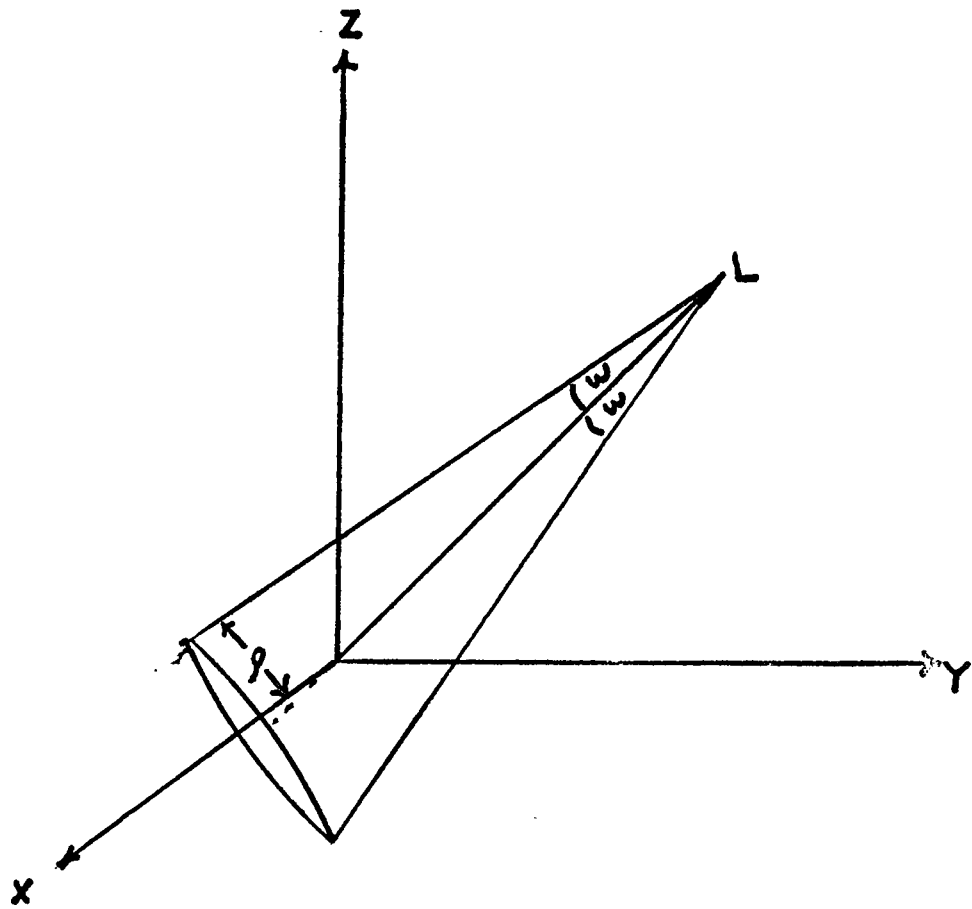
To quote from Uebel and Wing⁸³:

"Clearly the generalized pseudocontact shift equation (equation 9) could in principle be solved, but the complexity of the problem, we feel, makes such solutions impractical. In addition to R and θ , one would need to know the three principal g values and an additional angle. The geometry of the complex with respect to the magnetic axes would also need to be known in order to evaluate the shifts. In the case of a fluxional complex, the calculated shifts would have to be averaged over all molecular orientations."

The Question of the Orientation of the Principal Magnetic Axis

The problem of orienting the principal magnetic axis has been investigated by J. D. Roberts⁸⁴ and R. J. P. Williams.⁸⁵ If the principal magnetic axis is not assumed to be collinear with the lanthanide-heteroatom bonds two additional parameters must be defined. These are two angles, the first a measure of the tilt of the magnetic axis off the lanthanide-heteroatom bond, and the second an angle which describes the precise location of the magnetic axis on the cone defined by the first angle. These two parameters are shown in Figure 4.

FIGURE 4: THE ORIENTATION OF THE PRINCIPAL MAGNETIC AXIS IN
THE LSR-SUBSTRATE COMPLEX



If the axially symmetric pseudocontact model is used along with these two additional angular variables, there are a total of six experimental parameters which must be derived. R. J. P. Williams et al.⁸⁵ have fitted the ^1H LIS data obtained by treating cholesterol with various $\text{Ln}(\text{DPM})_3$ chelates to the axially symmetric pseudocontact model containing a magnetic axis that was not defined to be collinear with the metal-oxygen bond. The principal magnetic axis was found to be collinear with the metal-oxygen bond to within 1° . Similar results have been obtained by Roberts⁸⁴ using the LIS ^1H data for borneol and isoborneol to fit the same model as above. Again the principal magnetic axis was found to be collinear to within about 2° with the metal-oxygen bond. It is clear that the principal magnetic axis in the LSR-substrate complex is effectively collinear with the heteroatom-lanthanide bond for at least these cases.

B. The Mathematical Model for the LSR-Substrate Interaction

The approach described in the following section has been the subject of two communications^{86,87} in the literature*. Other workers have also discussed the effects responsible for the signal dispersion in terms of a contact shift, a pseudocontact shift or a combination of the two effects.^{88,89} Many recent applications have been qualitative in nature. In addition some groups have attempted to use a quantitative approach to treat the experimental data. For example, Briggs et al.⁷⁵

*The title of these communications are "Interpretation of the Pseudocontact Model for Nuclear Magnetic Resonance Shift Reagent. I. The Agreement Factor, R and II. Significance Testing on the Agreement Factor, R."

have fitted the ^1H data for borneol in the presence of $\text{Pr}(\text{DPM})_3$ to the axially symmetric pseudocontact equation. Farid, Ateya and Maggio⁷⁶ used the ^1H $\text{Eu}(\text{DPM})_3$ data for adamantan-2-ol, trans-4-tert-butylcyclohexanol and two rigid ethers to fit equation (8), the axially-symmetric pseudocontact model. Huber and Pascal⁹⁰ have analyzed the $\text{Eu}(\text{DPM})_3$ ^1H data for quinoline, isoquinoline and benzo[f]quinoline with respect to the pseudocontact model. Demarco et al.⁹¹ have carried out an analysis on the $\text{Eu}(\text{FOD})_3$ and $\text{Eu}(\text{DPM})_3$ ^1H data for ten monofunctional cyclic substrates having various different functional groups. Angerman et al.⁹² have carried out computer analyses of the $\text{Pr}(\text{DPM})_3$ ^1H data for chloroquine using the dipolar shift equation, equation (8). Randall and Moss¹⁴ have also developed a computer assisted method for analyzing LIS data based on equation (8).

Our approach to the quantitative treatment of data from LIS experiments is based on the conclusions reached in the earlier sections. Based on both chemical information as well as considerations of statistical economy, we make the assumption that the axially symmetric form of the pseudocontact shift expression is applicable to at least proton shifts in NMR experiments. Moreover, the principal magnetic axis is defined to be collinear with the metal-heteroatom bond in our scheme. For ease in calculation, a molecule is described with respect to an internal Cartesian coordinate system with the heteroatom at the origin (Figure 3). The lanthanide, L, is then moved incrementally over the surface of a sphere of radius d , the assumed heteroatom-lanthanide bond distance. The location of L on the sphere is described in terms of the two angles,

θ (the colatitude, measured from the positive Z axis) and Ω (the azimuth, measured counterclockwise from the X-Y plane), as shown in Figure 3. At each lanthanide position, the variable term

$$(3\cos^2\theta_i - 1)/r_i^3$$

in the pseudocontact equation is evaluated for all i protons. This set of numbers is then scaled by least squares against the relative observed shifts $(\Delta H/H)_{oi}$ to yield a set of calculated shifts $(\Delta H/H)_{ci}$. In order to assess the correspondence between the observed and calculated values, an agreement factor, R , is evaluated as

$$R = \left[\frac{\sum_i ((\Delta H/H)_{oi} - (\Delta H/H)_{ci})^2 w_i}{\sum_i (\Delta H/H)_{oi}^2 w_i} \right]^{1/2}$$

Table VII shows minimum agreement factors obtained for several oxygenated substrates. Each substrate is a molecule of known stereochemistry for which proton assignments were either available or made easily.

The endo-norborn-5-en-2-ol substrate can be used to illustrate several interesting features of our computational method. Table VIII gives the observed and calculated shifts for the endo-norbornenol. The lanthanide position corresponding to a best fit (minimum, R)* for the norbornenol is at $d = 3.2 \overset{\circ}{\text{A}}$, $\theta = 50^\circ$ and $\Omega = 290^\circ$. This structure is shown in Figure 5. Note that the lanthanide position is chemically sensible. However, can one be sure that this minimum R value does not

*This minimum R (MINR) was obtained using equal weighting factors.

TABLE VII
MINIMUM AGREEMENT FACTORS OBTAINED FOR OXYGENATED
HYDROCARBONS

Compound	R
<u>cis-4-tert-Butylcyclohexanol</u> ^(a)	0.043
<u>trans-4-tert-Butylcyclohexanol</u> ^(a)	0.081
Norcamphor ^(b)	0.074
<u>endo-Norborn-5-en-2-ol</u> ^(b)	0.034
Borneol ^(a,b)	0.081
Isoborneol ^(a,b)	0.050
Bicyclo[3.2.0]hept-3-en-2-one ^(c)	0.060
5-Methylbicyclo[3.2.0]hept-3-en-2-one ^(c)	0.080
Andamantan-2-ol ^(d)	0.032
Cyclooctatetraene dimer epoxide ^(e)	0.092

(a) P. V. Demarco, T. K. Elzey, R. B. Lewis, and E. Wenkert, J. Amer. Chem. Soc., 92, 5734 (1970).

(b) The experimental LIS data for these compounds are given in Appendix A.

(c) Compound obtained from Professor R. L. Cargill, University of South Carolina. The LIS data for these compounds is also presented in Appendix A.

(d) G. H. Wahl and M. R. Peterson, Chem. Commun., 1167 (1970).

(e) M. R. Willcott, J. F. M. Oth, J. Thio, G. Plincke, and G. Schroder, Tetrahedron Lett., 1579 (1971).

TABLE VIII
COMPARISON OF OBSERVED AND CALCULATED LANTHANIDE-INDUCED CHEMICAL
SHIFTS FOR THE SYSTEM: $\text{Eu}(\text{DPM})_3$ -endo-NORBORN-5-EN-2-OL

Proton	Obsd.	Calcd.
1	11.0	9.9
2	22.8	23.0
3-endo	15.2	15.2
3-exo	10.2	10.1
4	5.3	5.7
5	6.0	6.1
6	8.0	7.9
7-syn	5.7	6.3
7-anti	4.8	4.4

FIGURE 5. endo-NORBORNENOL AS DESCRIBED WITH RESPECT TO THE
INTERNAL COORDINATE SYSTEM

Oxygen is at the origin, the O-C-2 bond is placed along the negative Z axis, and atom C1 is placed in the X-Z plane with the positive X coordinate.

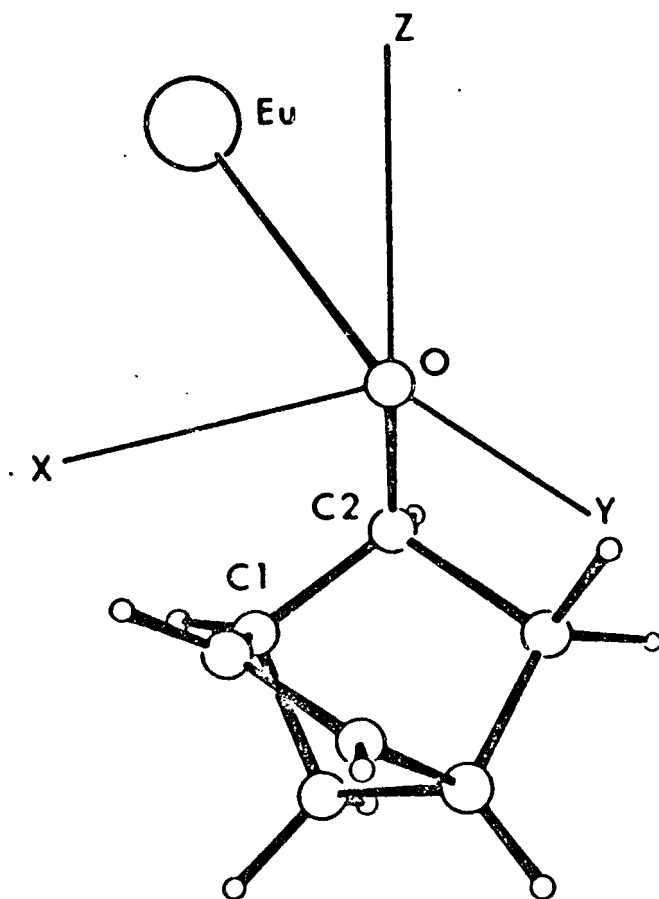


Figure 5. *endo*-Norbornenol as described with respect to the internal coordinate system. Oxygen is at the origin, the O-C-2 bond is placed along the negative *Z* axis, and atom Cl is placed in the *X-Z* plane with the positive *X* coordinate.

FIGURE 6. PLOTS OF THE AGREEMENT FACTOR R FOR endo-NORBORNENOL

Assumed O-Eu distances are, top to bottom, 2.9, 3.1, and 3.3 Å. In each case, contours are at intervals of 0.02 in R, with the outer contour at R = 0.12.

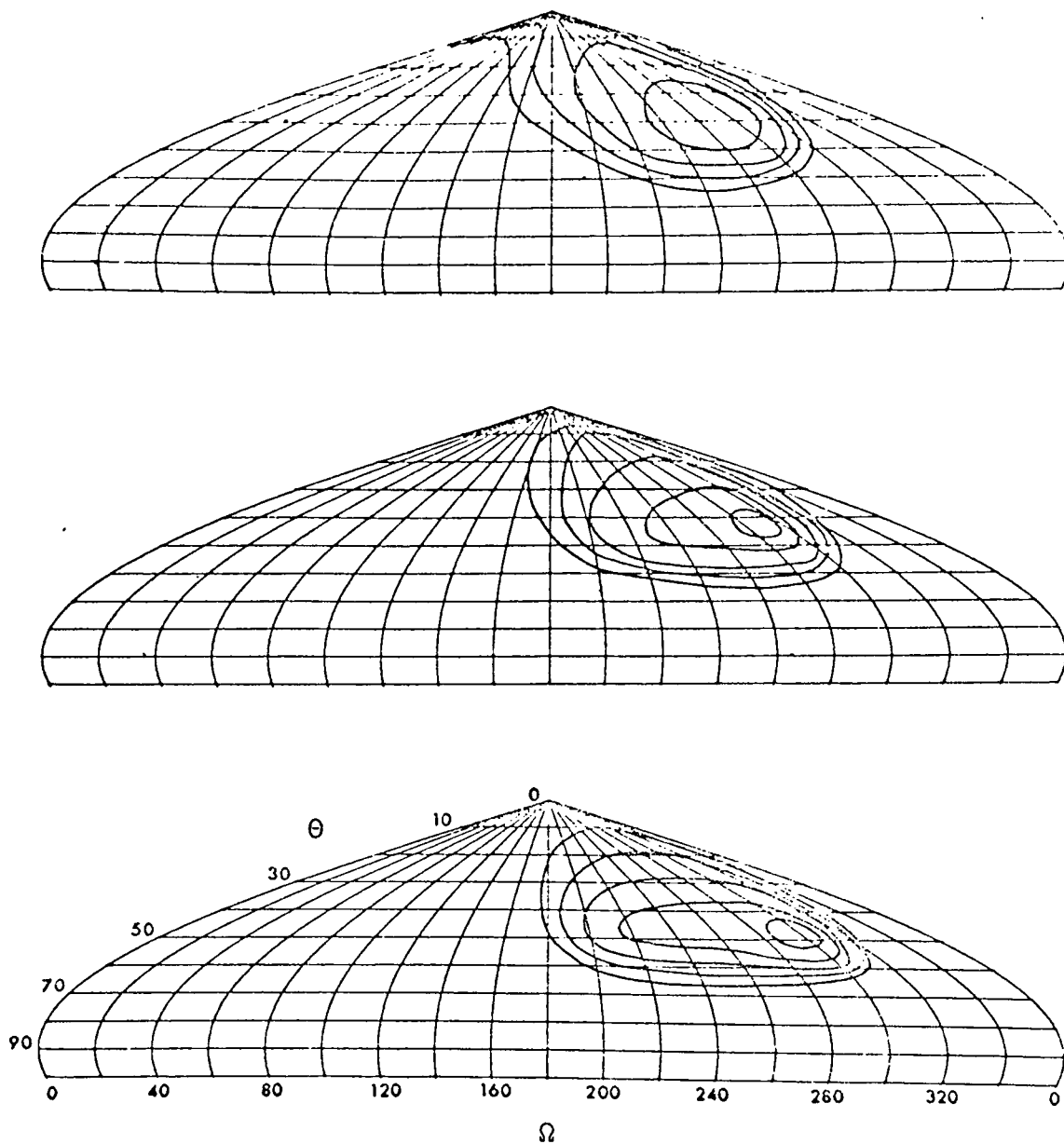


Figure 6. Plots of the agreement factor R for *endo*-norbornenol. Assumed O-Eu distances are, top to bottom, 2.9, 3.1, and 3.3 Å. In each case, contours are at intervals of 0.02 in R , with the outer contour at $R = 0.12$.

represent a local minimum rather than a real minimum? This question can be answered by displaying the values of R as a function of θ and Ω for a given lanthanide-oxygen bond distance on a map projection, such as the Samson-Flamsteed sinusoidal equal area projection.⁹³ Figure 6 illustrates this procedure. In Figure 6, the lines represent lines of equal minimum R values.

The goodness of fit, in general, for the compounds described in Table VII are quite insensitive to the value assumed for the lanthanide-oxygen distance and the map projections for these compounds reveal a single smooth minimum in R for all distances between 2.5 Å and 3.5 Å. Several features of our approach which can be of great utility have already been discussed in the communication titled "Interpretation of the Pseudocontact Model for Nuclear Magnetic Resonance Shift Reagents. I. The Agreement Factor, R ."⁸⁶ Quoting from this report:

"(1) The geographer's plot provides a visual description of the agreement factor, permitting rapid appraisal of the effects of altering the computational parameters. (2) Internal coordinates determined from molecular models (e.g., Dreiding) can be used without jeopardizing the method. Errors of ca. 0.1 Å cause changes of less than 0.01 in R . (3) Since calculated values are scaled to observed, we only require relative induced chemical shifts. (4) The method is rapid. When data of reasonable precision are used directly, the nmr measurements, calculations, and interpretation require about 2 man-hr. (5) The insensitivity of R to most variables except structure and signal assignment make it a useful assessing function."

Significance Testing on the Agreement Factor, R

Hamilton has investigated the reliability of hypothesis regarding the results of crystallographic studies, by the use of significance tests on the crystallographic R factor.^{94,95} Willcott and Davis has shown that the same kind of significance test can be carried out using the LIS minimum agreement factor, MINR.⁸⁷ Willcott and Davis note that the MINR value corresponds to a least-squares best fit of a particular model and therefore, can be used in the hypothesis testing schemes described by Hamilton.

Briefly, the procedure is as follows. First, one obtains a set of LIS shift indices for the compound in question. Then, one fits the LIS data to one of several structural models, each of which is characterized by a minimum R. The statistical testing of one model against another is accomplished by applying the R ratio test to determine the confidence at which one model may be rejected in favor of another.^{94,95} Rejection of a hypothesis at a given confidence level $\alpha\%$ means that one risks rejecting a true hypothesis $\alpha\%$ of the time. Several illustrative examples follow.

Treatment of the $^1\text{H Eu}(\text{DPM})_3$ LIS indices for isoborneol* with the isoborneol structure generates an R factor of 0.05. When these data are fitted with the borneol structure, a minimum R value of 0.445 is obtained. An hypothesis can be formulated in the following way; the borneol structure gives as good agreement with the data as the

*These indices can be found in Appendix A.

isoborneol structure. There are 11 observations (^1H shift indices) in this system, while 4 experimental parameters (3 positional parameters for the lanthanide and the scaling factor K , between the observed and calculated LIS indices) are unknown. The number of degrees of freedom is $11-4 = 7$. Reference to Hamilton's tables, shows that the minimum R factor ratio for rejecting this hypothesis at the 0.5% level is 1.822. The observed R factor ratio is $0.445/.05 = 8.90$. Clearly, this hypothesis can be rejected.

A similar analysis of the pmr $\text{Eu}(\text{DPM})_3$ borneol spectrum gives minimum R values of 0.081 for the borneol coordinates and 0.351 for the isoborneol coordinates. The hypothesis to be tested is: the isoborneol structure is in as good agreement with the data as is the borneol structure. The observed R-factor ratio is $0.351/0.081 = 4.33$, clearly much in excess of the minimum value of 1.822 necessary to reject the hypothesis at the 0.5% level.

In one of our early attempts to fit the LIS spectrum of 5-methylbicyclo[3.2.0]hept-3-en-2-one (I) the methyl group was misplaced at



carbon 1 (II), giving a best fit of $R = 0.129$. When the methyl group was correctly placed at carbon 5, the R value obtained was 0.080.

The 1-methyl possibility can be rejected in favor of the 5-methyl isomer at about the 5% level, using the significance tests.

This method of significance testing provides a qualitative assessment of how well a given set of LIS indices matches one of several structures. Note however, that this method does not provide us with the best possible structure. It can provide us with a clear choice of the best of several models we are testing. This computational method does not take any chemical information, other than the LIS indices, into account. For example, the Eu-O bond distance, corresponding to a best fit in compound II was 2.0 Å. This short bond distance is in conflict with our chemical experience in such systems.

In summary, we have constructed a model for the LIS experiment. The computational method outlined provides a rapid means of assessing how well a given structure matches a set of experimentally determined LIS indices. The agreement factor, R, provides a means for the statistical testing of the goodness of fit of several structures to a given set of data. This method meets the requirements set out in Chapter II. It has been our experience that, in over fifty compounds, this method has generated the correct structure for the compound in question.

CHAPTER VI

APPLICATIONS OF THE PSEUDOCONTACT MODEL TO LIS EXPERIMENTS

VI. APPLICATIONS OF THE PSEUDOCONTACT MODEL TO LIS EXPERIMENTS

A. Extension of the Computational Method to ^{13}C LIS Spectra

The advantages of the pseudocontact model, described in the previous chapter in matching experimental ^1H LIS data with structures, have already been enumerated. On the basis of statistical considerations, the greater number of observations realized by using ^{13}C LIS data, as well as ^1H data, to describe a substrate, increases the confidence levels at which structures can be tested. In order to apply the pseudocontact model to ^{13}C LIS data, the following questions must be considered.

- (1) Are the ^{13}C $\text{Eu}(\text{DPM})_3$ shift indices completely pseudocontact in origin?
- (2) If not, can these ^{13}C shift indices be factored into a contact term and a pseudocontact term?
- (3) Is there a lanthanide shift reagent which generates ^{13}C data which is largely, if not completely pseudocontact in origin?

Discrepancies in $\text{Eu}(\text{DPM})_3$ - ^{13}C Spectra

Weissman has cautioned that both contact shifts and pseudocontact shifts are to be expected when using europium shift reagents.⁹⁶ The iterative computational scheme described in the previous section has been shown to reproduce proton shift behavior to a high degree of precision (see Table VI). This same observation has been made in other laboratories.^{75,76,84,91,92} The duplication of ^{13}C data by this method seems less satisfactory.^{97,98,99}

In 1971, we determined both the ^1H and ^{13}C LIS indices for borneol and isoborneol using $\text{Eu}(\text{DPM})_3$.⁹⁷ These data are presented in Appendix A. The minimum R values obtained on the ^1H indices for both compounds were shown in Table VII. They are,

	isoborneol	borneol
R	.05	.081

The minimum R values were obtained on the corresponding ^{13}C LIS indices for these compounds. These R values were both around .20. Moreover, the lanthanide positions corresponding to the best fit for the ^{13}C data did not match the positions corresponding to a best fit for the ^1H data.

Roberts⁹⁸ has observed anomalous shifts in several amine systems, the most spectacular of which, is an upfield shift of considerable magnitude in the β -carbon of the norbornylamine- $\text{Eu}(\text{FOD})_3$ system. Cushley⁹⁹ has noted that the ^{13}C LIS data for three primary amines with $\text{Eu}(\text{FOD})_3$ were upfield at the β -carbon, while all other shifts were downfield. No amount of adjustment in the pseudocontact model can replicate the total behavior of these systems, so a semi-qualitative description was reached by postulating a large ^{13}C contact shift when the LSR is a europium LSR. Theory presented by Reuben¹⁰⁰ and ^{14}N LIS studies¹⁰¹ can be combined to predict an upfield shift at the β -carbon of these systems along with an attenuated contact shift in the ^1H spectrum at all positions of europium.

A series of LIS experiments, using $\text{Eu}(\text{DPM})_3$ as the LSR and several pyridine bases as substrates, were performed in an attempt to determine the magnitude and sign of the ^{13}C contact shifts. Pyridine bases have been demonstrated to be sensitive to contact shifts by both Dodrell and Roberts¹⁰² as well as Morishima *et al.*¹⁰³ The pyridine bases examined were pyridine, 2,6-lutidine, 2,4,6-lutidine, 3,4-lutidine, quinoline and isoquinoline. The ^1H and ^{13}C shift indices of these bases were obtained on the same samples of these pyridine bases. The exact experimental procedure for these experiments is given in Appendix B.

The computation method was altered in such a way that

- (i) the europium location was mapped against the agreement factor, R, for the ^1H data;
- (ii) the scale factor, K, in the equation

$$\frac{\Delta\text{H}}{\text{H}} = \text{K} \left(\frac{3\cos^2\theta - 1}{r^3} \right)$$

used to match experimental shifts to calculated shifts was recorded;

- (iii) the carbon pseudocontact shift values were computed for each europium location using the scale factor K; and
- (iv) a difference spectrum (observed-calculated) was generated for the carbon spectrum.

The results of the experiments are shown in Table IX. Pyridine can be used to illustrate the procedure. Systematic variation of the

europium location over the surface of spheres of radius 2.0-5.0 Å centered on the pyridine nitrogen in 0.1 Å steps showed R factors ranging from 2.25% (2.0 Å) to 6.0% (5.0 Å). Over the range 3.2-3.6 Å, numerous regions were found for the lanthanide which gave R factors of less than 2%. In this range the best agreement, R = 1.67%, was noted at 3.4 Å. Even though we anticipated the europium would lie along the C₂ axis through the nitrogen atom of pyridine, the minimum R factors were obtained when the Eu atom was displaced ca. 30° from the C₂ axis and ca. 40° from the plane of the ring. This unexpected result may be an artifact of our computational approach, or it may be due to experimental error, or a combination of both factors. In any event, the europium angular location was found to influence the R factor much less than the Eu-N distance. This rather long Eu-N distance, in our experience and in that of Hawkes, Marzin, Johns, and Roberts,⁹⁸ almost certainly arises from contact contributions to the proton spectrum. At the location corresponding to a minimum R, a difference spectrum ($^{13}\text{C}_{\text{obs}} - ^{13}\text{C}_{\text{calc}} = ^{13}\text{C}_{\text{difference}}$) was obtained. It is included in Table IX. Corresponding difference spectra were obtained for all europium locations with R < 2.0% and a considerable range of absolute $^{13}\text{C}_{\text{diff}}$ was noted. However, the difference spectra can be expressed as relative spectra, obtained by setting any desired $^{13}\text{C}_{\text{diff}}$ (say C-α) at 1.0 and scaling the other shifts to it. Even though the absolute values of the carbon discrepancies differ by as much as 30%, the relative values of $^{13}\text{C}_{\text{diff}}$ remain nearly constant.

Analogous ^{13}C difference spectra were obtained for five additional pyridine bases. Table IX lists the N-Eu distance for the minimum R obtained from the ^1H data. The set of magnitudes of the calculated carbon difference shifts obtained for the minimum R position, as well as the relative shifts, can also be found in Table IX. Several important features are obvious from the pyridine base data. First, the ^{13}C paramagnetic induced shifts cannot be replicated by any simple pseudocontact model. This model would have to explain not only the magnitudes of the ^{13}C shifts relative to ^1H , but also the alternation of the sign (minus, plus, minus; α , β , γ) of the effect in ^{13}C . Second, the ^1H spectrum cannot be free of a contact contribution, but it is free enough that small agreement factors are obtained. Third, the precise location of the metal is materially and understandably dependent on the substituent pattern. The three least hindered nitrogens (pyridine, 3,5-dimethylpyridine, isoquinoline) all have a minimum R factor for Eu-N distances ca. $3.2 \overset{\circ}{\text{A}}$, while the more hindered ones (2,6 and 2,4,6 methyl derivatives and quinoline) show minima at ca. $4.4 \overset{\circ}{\text{A}}$. The somewhat long $3.2 \overset{\circ}{\text{A}}$ Eu-N distance is attributed to contact contributions to the proton spectra. We emphasize, however, that the attendant drop in the magnitude of the observed shifts with increased steric hindrance cannot of itself be used to deduce the europium location. Indeed, location of the lanthanide may be accomplished efficiently only by some type of iterative minimization procedure. The coincidence of smaller

shifts and larger Eu-N bond distances in the present case is likely fortuitous. For instance, shift values will depend on the magnitude of the europium-substrate formation constant among other factors.

The most striking aspect of the ^{13}C difference spectra defined earlier is the regular alternation of signs of the difference shifts in the heterocyclic ring, viz. -, +, - at C- α,β,γ . Similar alternation of precisely reversed sign order has been noted by Doddrell and Roberts¹⁰² as well as Morashima et al.¹⁰³ for pyridine base adducts of bis-(acetylacetonato)Ni(II). Polarization leaving β spin in the ring has been predicted¹⁰⁴ to occur for the lanthanides and could provide a ready explanation for this sign reversal if the Ni spin is α . The sign alternation has been examined theoretically and was attributed to spin delocalization in the σ bond molecular framework, with the further assumption of excess α spin for Ni(II) complexes.^{105,106,107} Additional evidence that this explanation is satisfactory in the present work is provided by the positive shift detected for methyl groups substituted in the 2,4,6 positions as well as the shifts measured in the benzenoid rings of quinoline and isoquinoline. Furthermore, large upfield shifts have been measured for heterocyclic, europium bonded nitrogens as might have been anticipated from the above discussion.¹⁰¹

Though the precise relationships among the magnitudes of the carbon shifts calculated are suspect due to inadequacies in the theory, we nevertheless feel compelled to compare our ^{13}C difference spectra with some quantitative predictions from INDO calculations. The calculated shift ratios for pyridine (assuming β spin) are -1:+0.58:-0.34 for the α, β, γ carbons which compares to our difference shift ratios of

-1:+0.70:-0.37.¹⁰⁵ Note that the ratios of the α , β , γ shifts were calculated using crystallographically determined pyridine bond distances. Small changes in these values cause large variations in the shift ratios. While this reasonable agreement may in some part be coincidental, resulting from experimental or theoretical errors, we will make use of ^{13}C difference maps as measures of the contact shift.

Is the proton data then properly treated as pseudocontact? The answer certainly is not precisely. We have observed that if small changes in the values for the proton chemical shifts are introduced into the R factor calculations, this does not effect a drastic alteration of the europium position (i.e. less than 10%). Moreover, shift ratios in the carbon difference spectra are not changed significantly. Attempts to improve the pseudocontact description of the proton data based on the ^{13}C contact shift have failed because we cannot determine a constant scaling factor between ^{13}C , ^1H shifts for the various CH bonds.

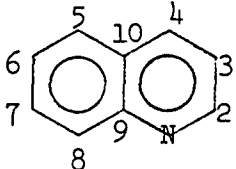
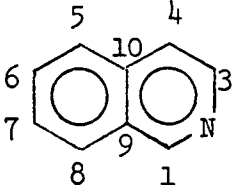
In summary, we are confident that $\text{Eu}(\text{DPM})_3$ interacts with pyridine type bases to produce both contact and pseudocontact shifts. The ^{13}C nmr data cannot be explained without specific inclusion of a large amount of contact shift. Indeed, we suggest that considerable confusion may result if the assignment of ^{13}C resonances is attempted from europium shifts alone,⁹⁷ especially when easily polarized molecules like pyridine are examined. On the other hand, the proton data even for the nitrogen heterocycles can be satisfactorily treated by the pseudocontact model.

TABLE IX
EXPERIMENTAL 1:1 Eu(DPM)₃:SUBSTRATE CHEMICAL SHIFTS OF SOME PYRIDINE BASES

	R	d(Eu-N) Å		¹ H _{obs}	¹ H _{calc}	¹³ C _{obs}	¹³ C _{calc}	¹³ C _{diff}	Relative ¹³ C _{diff}
Pyridine	0.9%	2.7	α	-31.02	-31.11	-90.00	-67.78	-22.22	-1.00
			β	-10.68	-10.59	+ 0.88	-24.33	+25.21	+1.13
			γ	- 9.71	- 9.33	-30.22	-18.73	-11.49	-0.52
2,6-Lutidine	5.7%	3.9	α			-15.80	- 9.09	- 6.71	-1.00
			β	- 2.60	- 2.77	- 0.90	- 4.41	3.51	.52
			γ	- 2.68	- 2.25	- 5.70	- 3.56	- 2.14	- .32
			α-CH ₃	- 5.20	- 5.20	-13.40	- 6.27	- 7.13	-1.06
2,4,6-Lutidine	5.4%	4.3	α			-12.30	- 4.85	- 7.45	-1.00
			β	- 1.43	- 1.60	2.07	- 2.45	4.52	.61
			γ			- 6.98	- 1.99	- 4.99	- .67
			α-CH ₃	- 3.37	- 3.28	-10.97	- 3.74	- 7.23	- .97
			γ-CH ₃	- 0.90	- 0.98	- 1.93	- 1.10	- 0.83	- .11
3,5-Lutidine	0.6%	2.8	α	-26.7	-26.66	-67.80	-51.66	-16.14	-1.00
			β			3.10	-19.44	22.54	1.40
			γ	- 7.50	- 7.55	-22.70	-14.95	- 7.75	- .48
			β-CH ₃	- 4.91	- 5.08	- 6.00	- 6.24	- 0.24	- .01

TABLE IX CONTINUED

EXPERIMENTAL 1:1 Eu(DPM)₃:SUBSTRATE CHEMICAL SHIFTS OF SOME PYRIDINE BASES

R	d(Eu-N) Å		¹ H _{obs}	¹ H _{calc}	¹³ C _{obs}	¹³ C _{calc}	¹³ C _{diff}	Relative ¹³ C _{diff}	
Quinoline 	4.7%	4.6	2	-22.52	-21.88	-69.4	-22.54	-46.86	-1.00
			3	- 6.38	- 7.44	- 4.8	-11.24	6.44	.14
			4	- 4.96	- 5.84	-18.18	- 8.88	- 9.30	.20
			5	- 4.04	- 4.68	- 7.16	- 6.42	- 0.74	.02
			6	- 3.34	- 3.48	- 7.10	- 5.42	- 1.68	.04
			7	- 5.36	- 4.10	-12.34	- 7.00	- 5.34	.11
			8	-19.0	-19.28	-38.00	-15.30	-22.70	.48
			9			-36.4	-19.32	-17.08	.36
			10			2.6	-10.56	13.16	.28
			Isoquinoline 	3.0%	3.2	1	-23.70	-23.78	-70.20
3	-25.70	-25.49				-64.00	-38.73	-25.27	.72
4	- 9.11	- 9.33				- 0.20	-16.60	16.40	.47
5	- 6.10	- 5.30				- 8.90	- 6.99	- 1.91	.05
6	- 3.40	- 3.46				- 2.80	- 5.04	2.24	.06
7	- 3.40	- 3.53				- 2.10	- 5.26	3.16	.09
8	- 5.80	- 6.54				-10.10	- 8.41	- 1.69	.05
9						- 3.60	-16.45	12.85	.37
10						-21.60	-13.29	- 8.31	.24

The Evaluation of Lanthanide Induced Carbon-13 Contact vs Pseudo-contact NMR Shifts

In the preceding section, a methodology was developed for generating a set of ^{13}C difference spectra. Evidence for viewing this $^{13}\text{C}_{\text{obs}} - ^{13}\text{C}_{\text{calc}}$ spectrum as an estimate of the amount of contact interaction was presented in the previous section. There is reason to believe, on the basis of simple theoretical considerations presented by Reuben,¹⁰⁰ that different lanthanide shift reagents will induce varying amounts of contact shifts in a given substrate system. The methodology developed in the section can, therefore, be applied to a set of matched ^1H and ^{13}C shifts for a given substrate to evaluate the amount of contact shift induced by various lanthanide shift reagents. The pyridine bases, which were examined in the previous section, have been shown to be sensitive to contact interactions,^{102,103} and can provide a good substrate system for investigation.

Isoquinoline was chosen as the substrate for an evaluation of the contact contribution induced by various LSRs because of the number of ^1H indices available (seven).

The computational scheme was altered as before, so that

- (i) the lanthanide location was mapped against the agreement factor, R, for the ^1H data,
- (ii) the scale factor, K, in the equation

$$\frac{\Delta\text{H}}{\text{H}} = \left(\frac{3\cos^2\theta - 1}{r^3} \right) K,$$

used to match ^1H experimental to ^1H calculated shifts was recorded,

- (iii) the carbon pseudocontact shift values for each lanthanide position were computed using the scale factor, and,
- (iv) a difference spectrum $^{13}\text{C}_{\text{observed}} - ^{13}\text{C}_{\text{calculated}}$ was generated for the carbon spectra.

The lanthanide shift reagents examined were $\text{Pr}(\text{DPM})_3$, $\text{Nd}(\text{DPM})_3$, $\text{Eu}(\text{DPM})_3$, $\text{Tb}(\text{DPM})_3$, $\text{Dy}(\text{DPM})_3$, $\text{Ho}(\text{DPM})_3$, $\text{Er}(\text{DPM})_3$ and $\text{Yb}(\text{DPM})_3$. The experimental details of the procedure for this investigation are given in Appendix B.

The observed and calculated values for the ^1H and ^{13}C LIS indices for isoquinoline are shown in Table X. By convention, all shifts induced in a downfield direction are negative while all upfield shifts are positive. A comparison of the ^1H observed values with the ^1H calculated values indicates that, for all the lanthanide chelates used, there is quite good agreement with the pseudocontact model. Earlier reference was made to the fact that anomalous ^{13}C shifts were observed at the β -carbon of several substrate systems. If a comparison of the ^{13}C data is made at the C-9 position, several obvious discrepancies can be found. For neodymium, there is an observed shift of +.01 ppm at the C-9 position, whereas the corresponding calculated shift is +15.39 ppm. For europium, the observed C-9 shift is -3.60 ppm, whereas the calculated shift is -16.45 ppm. Holmium shows a C-9 shift of +.01 ppm whereas the corresponding calculated shift is 134.21 ppm. From even this preliminary comparison of the data in Table X, we can conclude that there are some

TABLE

OBSERVED AND CALCULATED 1:1 ^1H AND ^{13}C LIS INDICES

Lanthanide		H_1 Indices						
		H_1	H_3	H_4	H_5	H_6	H_7	H_8
Pr	obs	45.70	42.20	19.10	9.90	6.40	6.40	10.70
	calc	45.59	42.13	18.50	10.47	6.56	6.42	11.71
Nd	obs	22.70	26.30	8.40	5.80	4.40	4.40	5.80
	calc	22.47	26.45	9.03	5.13	3.42	3.56	6.60
Eu	obs	-23.70	-25.70	-9.11	-6.10	-3.40	-3.40	-5.80
	calc	-23.61	-25.68	-9.26	-5.26	-3.45	-3.53	-6.55
Tb	obs	393.20	372.30	131.10	63.90	42.50	42.50	79.60
	calc	392.76	373.16	132.69	65.59	37.13	36.29	79.04
Dy	obs	390.80	377.50	106.50	54.80	32.00	32.00	73.80
	calc	386.97	380.60	110.46	49.68	27.57	30.11	77.63
Ho	obs	171.20	163.30	58.30	27.90	15.00	15.00	27.90
	calc	170.19	163.13	60.29	29.07	15.57	13.91	29.62
Er	obs	-106.60	-113.30	-38.70	-21.70	-12.95	-12.95	-25.30
	calc	-106.99	-112.61	-39.35	-20.78	-12.77	-13.02	-26.44
Yb	obs	-75.60	-74.90	-26.90	-16.00	-9.50	-9.50	-17.60
	calc	-75.60	-74.63	-27.52	-14.43	-8.62	-8.41	-17.12

X

FOR ISOQUINOLINE WITH EIGHT LANTHANIDE SHIFT REAGENTS

^{13}C Indices								
C_1	C_3	C_4	C_5	C_6	C_7	C_8	C_9	C_{10}
100.00	94.00	28.20	12.00	11.00	9.80	11.10	25.50	30.50
88.06	93.21	36.85	14.34	9.90	10.15	16.81	37.34	29.63
69.50	60.30	10.70	4.90	6.00	2.10	7.90	.01	18.20
31.71	36.73	15.79	6.74	4.92	5.18	8.19	15.39	12.56
-70.20	-64.00	-.20	-8.90	-2.80	-2.10	-10.10	-3.60	-21.60
-34.09	-37.40	-16.25	-6.91	-5.00	-5.22	-8.33	-16.06	-13.00
624.70	573.10	329.50	99.80	59.40	97.00	97.30	355.90	157.60
774.53	825.75	304.62	97.68	62.06	64.32	120.48	310.11	236.43
679.0	582.00	339.00	118.80	69.90	95.20	108.70	317.00	208.40
736.60	855.81	294.45	82.15	50.52	55.48	112.90	300.43	223.20
275.80	281.00	153.20	47.80	28.30	37.00	53.50	.01	80.10
348.52	343.76	132.26	42.32	26.12	26.06	49.37	134.21	102.44
-211.80	-190.30	-42.00	-30.67	-26.29	-21.50	-36.14	-45.0	-68.57
-172.23	-180.87	-77.49	-28.94	-19.77	-20.76	-35.68	-77.16	-60.93
-134.40	-119.80	-50.10	-19.70	-15.20	-16.80	-26.90	-47.00	-41.70
-118.62	-119.67	-51.70	-19.71	-13.32	-13.37	-23.78	-52.13	-40.96

anomalous carbon-13 shifts observed with some of LSRs used while all the ^1H shifts seem well behaved.

Table XI shows the agreement factors obtained on only the ^1H data in column I. All the proton data seems to fit the pseudocontact model reasonably well with the worst fit being around .05. Column III contains the combined agreement factors obtained for all the shift data (^1H and ^{13}C). Note that there is quite a large variation in this combined agreement factor. Europium has a combined agreement factor of around .50 while ytterbium has a combined agreement factor of .04. The combined agreement factor for ytterbium approaches the agreement factor obtained using only the ^1H data. There is also a fairly large variation in the lanthanide nitrogen bond distance. As in the preceding section, this variation may be a reflection of some contact shifts in the ^1H data.

Table XII shows the $^{13}\text{C}_{\text{diff}}$ values obtained for the various LSRs. In all cases, except Ho, there is the same alternation of sign that was observed with the other pyridine bases in the preceding section. There is no reasonable explanation at this time, for the anomalous behavior of Ho. In the previous section, evidence was presented for viewing this $^{13}\text{C}_{\text{diff}}$ spectra as an estimate of the contact shift induced at a particular carbon. Morishima *et al.*¹⁰³ as well as Dodrell and Roberts¹⁰² have attempted to analyze the contact shifts induced in pyridine type systems by Ni(II) and Co(II). The analysis is complicated by the fact that contact interaction can occur by two different

TABLE XI
 MINIMUM PROTON R FACTORS, LANTHANIDE NITROGEN
 DISTANCES, AND COMBINED ^{13}C -H R FACTORS

Lanthanide	$R_{\text{H}}^{(a)}$	d (Å)	$R_{\text{C,H}}^{(b)}$
Eu	.030	3.1	.477
Nd	.048	3.3	.468
Er	.011	3.0	.176
Tb	.015	2.6	.269
Ho	.013	2.6	.333
Pr	.020	2.5	.116
Dy	.018	2.7	.300
Yb	.014	3.1	.040

(a) R_{H} is the agreement factor obtained for just the ^1H shift data.

(b) $R_{\text{C,H}}$ is the value which results from using all of the carbon and proton shifts when the lanthanide is located to minimize the proton R factor.

TABLE XII
 ^{13}C DIFFERENCE SPECTRA FOR THE NITROGEN RING OF ISOQUINOLINE

Lanthanide	$^{13}\text{C}_{\text{diff}}$ (a)					$^{13}\text{C}_{\text{diff}}/^{13}\text{C}_{\text{calc}}$				
	C_1	C_3	C_4	C_9	C_{10}	C_1	C_3	C_4	C_9	C_{10}
Pr	11.94	.79	-8.65	.87	-11.84	.13	.01	.31	.03	.46
Nd	37.79	23.57	-5.09	5.64	-15.38	.54	.39	.48	.31	---
Eu	-34.87	-25.27	16.40	8.31	12.85	.51	.42	.80	.40	3.42
Tb	-149.83	-252.65	24.88	-78.83	45.79	.24	.44	.08	.50	.13
Dy	-57.00	-280.21	44.55	-14.80	16.57	.05	.66	.13	.07	.05
Ho	-72.72	-62.76	20.94	-22.34	-134.0	.26	.22	.14	.28	---
Er	-39.57	-.43	35.49	-7.64	32.57	.19	---	.84	.11	.71
Yb	15.9	0.1	-1.6	0.74	-5.1	.12	---	.03	.02	.11

(a) $^{13}\text{C}_{\text{diff}} = ^{13}\text{C}_{\text{obs}} - ^{13}\text{C}_{\text{calc}}$.

mechanisms; (1) the spin delocalization mechanism and (2) the spin polarization mechanism. Further complication arose from the fact that contact shift can result from interactions involving π and σ type orbitals on both the metal and substrate. The sign and magnitude estimated for each of these contributions by Morishima¹⁰³ and Roberts¹⁰² are not intuitively obvious. Also the information extracted from an analysis of the contact shifts contains little information concerning the LSR-substrate topology. For these reasons, no analysis of the contact shifts in this system was attempted.

For the reasons presented, the $^{13}\text{C}_{\text{diff}}$ spectra was used only to estimate the relative magnitude of the contact interaction for each LSR examined. Earlier, Reuben¹⁰⁰ estimated the values of $\delta_{\text{pseudocontact}}/\delta_{\text{contact}}$ for various lanthanides. The value $^{13}\text{C}_{\text{diff}}/^{13}\text{C}_{\text{calc}}$ provides an experimental estimate of the values of $\delta_{\text{contact}}/\delta_{\text{pseudocontact}}$ around the nitrogen ring in isoquinoline. These values are shown in Table XII. In order to compare the values of $\delta_{\text{pseudocontact}}/\delta_{\text{contact}}$ with Reuben's values for each LSR used, the ^{13}C values obtained round the pyridine ring were averaged and the reciprocal of this average taken. This data is presented in Table XIII along with Reuben's "theoretically" estimated data. Note that there is rather close agreement between the experimental values and the theoretical values. It is clear from the isoquinoline data presented, that $\text{Yb}(\text{DPM})_3$ in at least nitrogen heterocyclic systems is the LSR

TABLE XIII
 AVERAGE VALUES FOR $\delta_{\text{PSEUDOCONTACT}}/\delta_{\text{CONTACT}}$ IN THE
 NITROGEN RING OF ISOQUINOLINE FOR EIGHT DIFFERENT LANTHANIDES

Lanthanide	δ_c/δ_p ^(a)	$(\frac{\delta_p}{\delta_c})_{\text{obs}}$ ^(b)	$(\frac{\delta_p}{\delta_c})_{\text{calc}}$ ^(c)
Pr	0.15	6.7	7.8
Nd	0.70	1.43	2.2
Eu	0.80	1.25	1.25
Tb	0.21	4.75	3.92
Dy	0.13	7.7	6.8
Ho	0.19	5.25	3.5
Er	0.25	4.0	1.9
Yb	0.05	20.0	11.0

(a) Obtained by averaging values for δ_c/δ_p in Table XII.

(b) Obtained by taking reciprocal of (a).

(c) Obtained by scaling Reuben's¹⁰⁰ values to Eu.

least likely to induce contact shifts. The following positive features of $\text{Yb}(\text{DPM})_3$ have been listed by Wolkowski *et al.*¹⁰¹ and Gansow *et al.*^{108,109} "(i) The induced shifts are downfield, facilitating interpretation of spectra. (ii) Little line broadening of either the carbon or proton resonances is observed. (iii) The proton shifts detected are ca. 300% larger than for $\text{Eu}(\text{DPM})_3$ at equal chelate concentrations. (iv) $\text{Yb}(\text{DPM})_3$ is suitable for use to determine structural features from dispersed carbon-13 spectra, $\text{Eu}(\text{DPM})_3$ is just as certainly not useful."

endo-Norborn-5-en-2-ol

One of the justifications for assuming that ^{13}C - $\text{Eu}(\text{DPM})_3$ data contained some amounts of contact interaction was the behavior of the isoborneol and borneol systems described earlier.⁹⁷ The large R factors obtained on the ^{13}C - $\text{Eu}(\text{DPM})_3$ indices compared with the R factors obtained on the corresponding ^1H -data coupled with the mismatch of lanthanide positions obtained from both sets of data (^{13}C and ^1H) led to a postulation of some contact shift in the ^{13}C data for both isoborneol and borneol. The endo-norbornenol system described in Chapter V was investigated by Willcott, Davis and Loeffler.¹¹⁰ A set of matched* ^{13}C and ^1H shift indices were obtained for $\text{Eu}(\text{DPM})_3$ and $\text{Yb}(\text{DPM})_3$. These data are given in Table XIV. There is quite good agreement between the ^1H observed and calculated values in the case of both LSRs. In fact,

*Matched by taking the spectra on identical samples.

TABLE XIV
 EXPERIMENTAL AND CALCULATED ^1H AND ^{13}C Eu(DPM) $_3$ AND Yb(DPM) $_3$

LIS INDICES FOR endo-NORBORN-5-EN-2-OL

	Eu		Yb			Eu		Yb	
	obs	calc	obs	calc		obs	calc	obs	calc
H ₁	15.6	15.0	37.0	37.5	C ₁	14.9	17.4	57.7	60.7
H ₂	34.1	34.6	88.6	87.9	C ₂	58.6	58.0	194.3	192.2
H ₃ X	13.2	12.7	33.4	33.6	C ₃	17.4	19.6	59.1	59.9
H ₃ N	22.4	22.3	56.2	56.0	C ₄	10.0	10.5	30.8	31.7
H ₄	7.6	7.7	19.7	20.0	C ₅	15.2	12.3	36.5	38.7
H ₅	9.4	9.4	22.6	23.9	C ₆	16.1	16.1	46.7	52.8
H ₆	14.7	13.8	34.5	34.7	C ₇	10.5	7.4	34.6	23.9
H ₇ S	7.8	8.8	22.2	22.3					
H ₇ A	7.1	7.4	18.5	18.6					

when the observed ^1H values for europium are least square fitted against the observed ^1H values for ytterbium, a MINR factor of 4% is obtained. This high fit factor indicates a quite good correlation between the two sets of data. When the same procedure is performed on the two sets of ^{13}C data, the R factor is 10%. Moreover, in Table XV the R factor obtained for the $\text{Eu}(\text{DPM})_3$ is much higher than that for the $\text{Yb}(\text{DPM})_3$ - ^{13}C data. The lanthanide positions corresponding to a minimum R value are also shown in Table XIV. The two positions corresponding to a best fit for the ^1H data are virtually the same. However, the lanthanide position corresponding to a best fit for both sets of ^{13}C data is considerably different. The Eu-oxygen bond distance obtained for the ^{13}C data is too short to be chemically reasonable. The $\text{Yb}(\text{DPM})_3$ - ^{13}C data generates a lanthanide position which is also considerably different than the position obtained for both sets of ^1H data. However, when the C_2 value is omitted in the computation, the Yb position obtained on the ^{13}C data becomes identical to both the ^1H positions. When the C_2 value is omitted in the europium computation, no improvement in the bond length is observed. The exclusion of the C_2 value does not seem to effect the lanthanide position markedly in the case of $\text{Eu}(\text{DPM})_3^*$. The low R factor obtained on the ^{13}C - $\text{Yb}(\text{DPM})_3$ data as well as the matching of lanthanide locations reinforces the view that $\text{Yb}(\text{DPM})_3$ is a superior shift reagent for use in ^{13}C LIS experiments.

*The two contour maps for the $\text{Eu}(\text{DPM})_3$ data, with and without C_2 , are virtually the same.

TABLE XV
 MINIMUM AGREEMENT FACTORS AND LANTHANIDE POSITIONS FOR
¹³C AND ¹H LIS INDICES OF endo-NORBORN-5-EN-2-OL

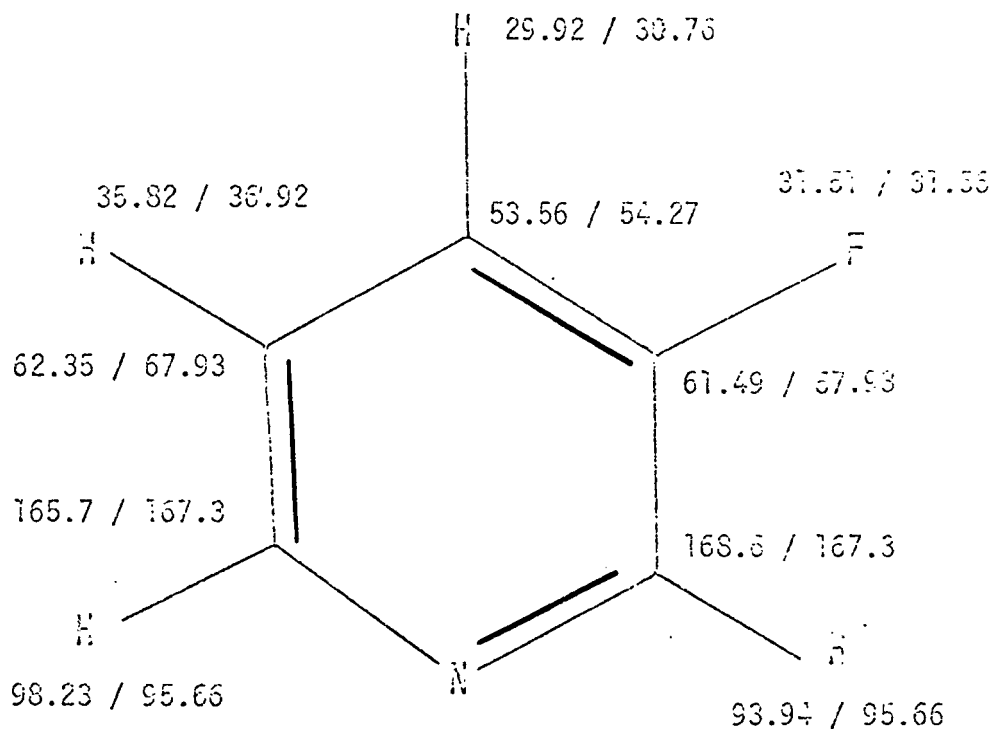
	Eu				Yb			
	R	d	θ	Ω	R	d	θ	Ω
¹ H	.033	3.0Å	50°	228°	.013	3.0Å	50°	250°
¹³ C	.08	2.0Å	70°	250°	.058	2.4Å	80°	236°
¹³ C (neglect- ing C ₂)	.15	2.0Å	70°	255°	.044	3.0Å	50°	228°

3-Fluoropyridine

Another example of the utility of $\text{Yb}(\text{DPM})_3$, as a shift reagent in LIS experiments on nuclei other than ^1H , is 3-fluoropyridine. The LIS indices for this compound were determined with both $\text{Eu}(\text{DPM})_3$ and $\text{Yb}(\text{DPM})_3$ by Willcott and Davis.¹¹¹ These values are shown in Figures 7 and 8. In Figure 8, the $\text{Eu}(\text{DPM})_3$ calculated values were determined by scaling the $\text{Eu}(\text{DPM})_3\text{-H}_4$ value to the $\text{H}_4\text{-Yb}(\text{DPM})_3$ value and then computing the values presented. There is good agreement between the observed and calculated values for all three nuclei (^{13}C , ^{19}F , ^1H) in Figure 7. In Figure 8 however, one of the β -carbons has an observed shift of -12.80 ppm while the calculated value is 25.97 ppm. The other β -carbon has an observed shift of -6.00 ppm while the calculated value is 25.99 ppm. The ^{19}F observed shift is 7.23 ppm while the calculated ^{19}F shift is 12.10 ppm.

From the results of these kinds of comparisons between $\text{Yb}(\text{DPM})_3$ data and $\text{Eu}(\text{DPM})_3$ data for the substrates presented, we can conclude that $\text{Yb}(\text{DPM})_3$ is a clear choice as the LSR most likely to produce ^{13}C shifts that fit the computational model we have developed. Because of this good fit, data from ^{13}C LIS experiments involving $\text{Yb}(\text{DPM})_3$ is be more useful in determining substrate topologies than data from $\text{Eu}(\text{DPM})_3\text{-}^{13}\text{C}$ LIS experiments.

FIGURE 7: THE OBSERVED AND CALCULATED $Y_b(\text{DPM})_3$ INDICES FOR
2-FLUOROPYRIDINE (from reference 111)



3 - FLUOROPYRIDINE

Yb(DPM)₃

OES / CAL

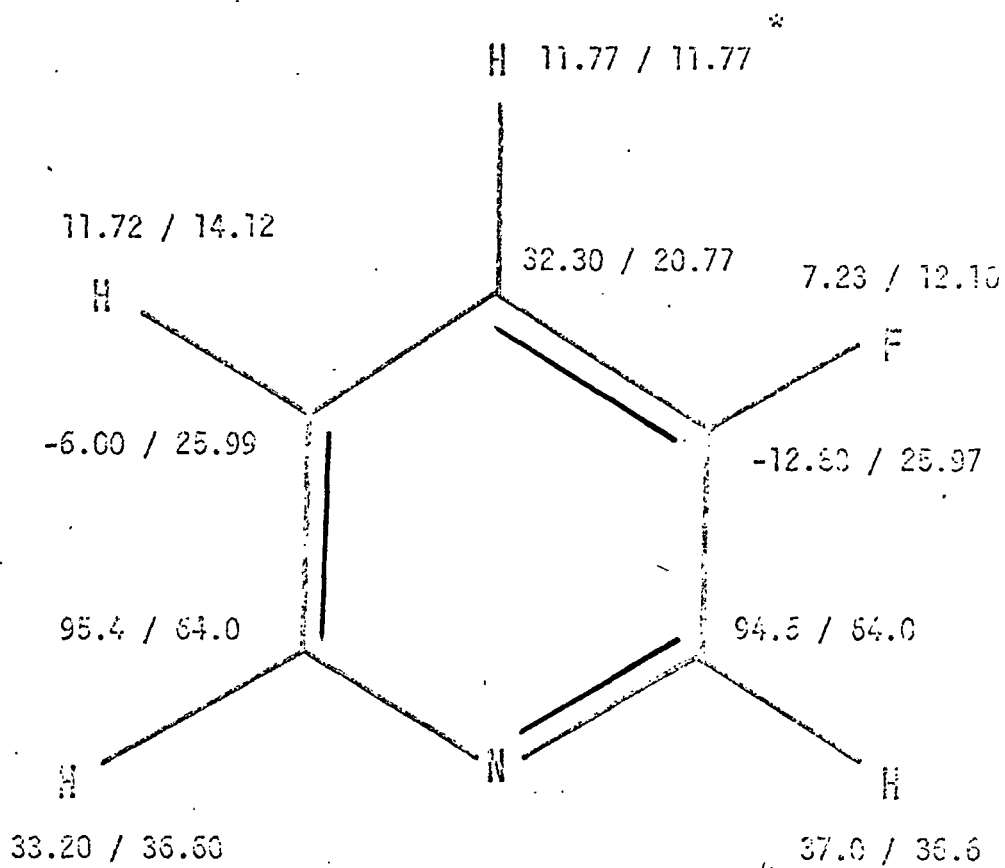
N-Yb = 2.5 A

R = 3.2 %

Wilcott

Davis

FIGURE 8: THE OBSERVED AND CALCULATED $\text{Eu}(\text{DPM})_3$ INDICES
FOR 2-FLUOROPYRIDINE (from reference 111)



3 - FLUOROPYRIDINE

Eu(DPM)₃

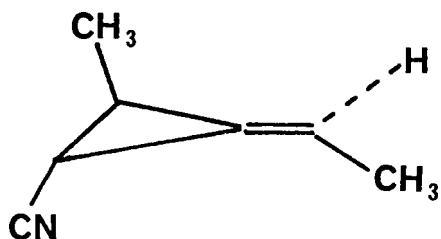
OBS / CAL

* (Cal from Yb position,
Scale to H 4)

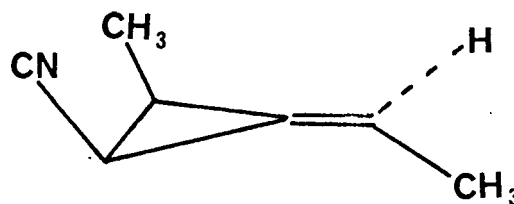
B. "Collinearity in the Structural Elucidation of Nitriles"*

Doering's Feist's Acid Derivatives

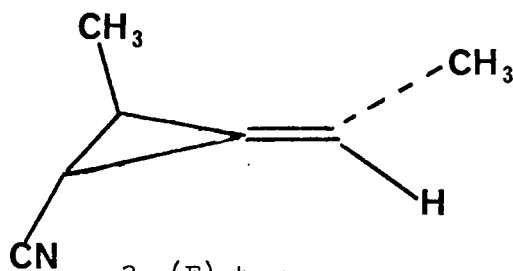
Doering and Birladeanu¹¹² have obtained four isomers of a Feist's acid derivative. These four isomers are shown below.



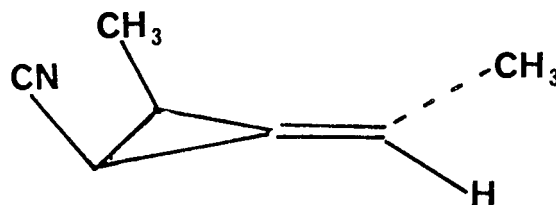
1 (Z)-trans



2 (Z)-cis



3 (E)-trans



4 (E)-cis

The methodology developed in Chapter V was applied to the LIS data (obtained by least squares treatment of the observed shifts for 6 or more $\text{Eu}(\text{FOD})_3$ dopings) for these compounds. These data are shown in Table XVI. Minimum values of R were obtained for all 16 combinations of the four structural possibilities with the four sets of experimental data. These minimum R values are shown in Table XVII, together with R factor ratios for the second best/best model. This

*A preliminary account of this work has been submitted for publication to the J. Amer. Chem. Soc. under the title "Interpretation of the Pseudocontact Model for NMR Shift Reagents VII. Collinearity in the Structural Elucidation of Nitriles." R. E. Davis, M. R. Willcott III, R. E. Lenkinski, W. Von E. Doering and L. Birladeanu.

system has five experimental observations and four parameters. There is therefore, one degree of freedom in this system. The lanthanide position at minimum R is less than 10° off the axis of the nitrile bond. Generally, all other positions, at the position corresponding to the second best R factor, for example, have a nitrile lanthanide bond angle larger than 30° . Imposition of the collinearity restraint on the four molecules, generates the sixteen MINR values shown in Table XVIII. By comparison the confidence levels for rejection of the hypothesis (the second best model fits the data as well as the best model) has increased from an average of 73% (no restraint) to 90% (collinearity restraint). The increased confidence level for each of the four individual hypothesis tests performed make the statistics for finding the four unique solutions corresponding to the four unique sets of data more secure.

Methylacrylonitriles

In an attempt to test the validity of the collinearity restraint used in the previous hypothesis testing, the $^1\text{H-Yb}(\text{DPM})_3$ LIS indices for the isomeric methylacrylonitriles shown below were obtained.

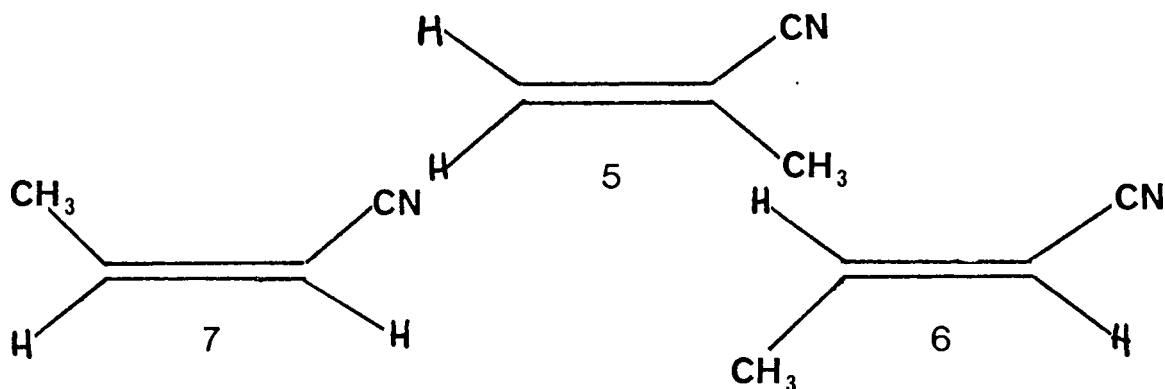


TABLE XVI

CHEMICAL SHIFTS AND OBSERVED AND CALCULATED RELATIVE SLOPES, COMPOUNDS 1-4 WITH $\text{Eu}(\text{FOD})_3$

Type of Hydrogen	1, (Z)-trans				2, (Z)-cis			
	Chem. Shift	(δ)	Relative Slopes		Chem. Shift	(δ)	Relative Slopes	
			Obs.	Calc. (a)			Obs.	Calc. (b)
H ₁	1.47		10.00	9.93	1.97		10.00	9.67
H ₂	1.99		6.19	6.13	2.02		4.06	4.78
(CH ₃) ₂	1.22		3.23	3.17	1.33		5.39	5.30
H _o	5.95		2.50	2.68	5.93		3.03	3.08
(CH ₃) _o	1.90		2.69	3.01	1.89		3.00	3.02

Type of Hydrogen	3, (E)-trans				4, (E)-cis			
	Chem. Shift	(δ)	Relative Slopes		Chem. Shift	(δ)	Relative Slopes	
			Obs.	Calc. (c)			Obs.	Calc. (d)
H ₁	1.48		10.00	9.83	1.96		10.00	9.88
H ₂	1.96		6.21	6.09	1.90		4.31	4.83
(CH ₃) ₂	1.24		2.66	3.17	1.37		5.31	5.04
H _o	6.00		3.53	3.70	6.06		3.51	3.51
(CH ₃) _o	1.84		1.47	1.56	1.84		1.59	1.59

(a)_R = 4.2%; (b)_R = 6.2%; (c)_R = 4.7%; (d)_R = 4.7%.

TABLE XVII

MINIMUM R VALUES (%) FOR BINARY COMBINATIONS OF MODELS 1-4
WITH SETS OF RELATIVE SLOPES, NO RESTRAINT OF
LANTHANIDE POSITION

	LIS Data Set			
	1	2	3	4
Model (Z)- <u>trans</u>	4.2	22.0	12.6	31.0
Model (Z)- <u>cis</u>	15.0	6.2	20.1	10.1
Model (E)- <u>trans</u>	13.2	25.7	4.7	20.1
Model (E)- <u>cis</u>	21.0	12.2	14.8	4.7
Ratio, $\frac{\text{Second best}}{\text{best}}$	3.14	1.96	2.68	2.14
Confidence level (%) for rejection of second best model	20 (80)	36 (64)	24 (76)	31 (69)

These data are shown in Table XIX. The procedure for obtaining these indices can be found in Appendix C. In this substrate system, there are three observed ^1H indices and the four parameters (r , θ , Ω , K) described earlier. There is, therefore, a minus one degree of freedom. Computation on this statistically meaningless basis, performed on the three isomers leads to the agreement factors and the lanthanide positions shown in Table XX.

Note that in testing Model 1- CH_3 against the three sets of data, there seem to be two minimum 0.3% and 3%. However, the 0.3% minimum is far off the linear nitrile lanthanide bond angle. Model cis-2-methyl seems to have two positions that generate reasonable fits. One at $2.8\overset{\circ}{\text{A}}$, a reasonable bond distance while the other occurs at $3.5\overset{\circ}{\text{A}}$, a bond distance which is too long to be chemically sensible. When the collinearity restraint is imposed on the system (the system now has one degree of freedom) the minimum R factors listed in Table XXI are obtained. Note that there is now only one minimum in the first row. However in order to make the hypothesis test more favorable in the Model cis-2- CH_3 case the additional chemical information concerning the long nitrogen-Yb bond must be applied. The imposition of the collinearity restraint in this system, again makes the statistical basis for the hypothesis testing more secure. The fact that the three model compounds which correspond to a best fit in this system are the three correct structures, seems to support the assumption of the collinearity restraint. Seux¹¹² et al. have imposed the collinearity restraint on

TABLE XVIII^(a)

MINIMUM R VALUES (%) FOR BINARY COMBINATIONS AS IN
TABLE XVII, WITH COLLINEARITY RESTRAINT

	LIS Data Set			
	1	2	3	4
Model (Z)- <u>trans</u>	8.3	27.0	13.4	26.9
Model (Z)- <u>cis</u>	22.3	6.5	26.0	12.0
Model (E)- <u>trans</u>	14.1	28.7	8.4	25.2
Model (E)- <u>cis</u>	25.8	12.6	22.7	6.7
Ratio, $\frac{\text{Second best}}{\text{best}}$	1.70	1.94	1.59	1.79
Confidence level (%) for rejection of second best model	10 (90)	7 (93)	11 (89)	8 (92)

(a) The hypothesis testing was performed on the four Feist's and derivatives shown on page 85.

TABLE XIX

CHEMICAL SHIFTS AND OBSERVED AND CALCULATED RELATIVE SLOPES,
METHYLACRYLONITRILE:Yb(DPM)₃, WITH COLLINEARITY RESTRAINT

Type of Hydrogen	Chem. Shift (δ)	Relative Slopes	
		Obs.	Calc. (a)
<u>1-Methylacrylonitrile</u>			
CH ₃	1.96	8.17	8.34
H ₁ - <u>cis</u>	5.74	10.00	10.10
H ₁ - <u>trans</u>	5.60	6.94	6.56
<u>cis-2-Methylacrylonitrile</u>			
CH ₃	2.04	6.59	6.74 ^(b)
H ₁	5.26	10.00	10.08
H ₂	6.46	5.83	5.49
<u>trans-2-Methylacrylonitrile</u>			
CH ₃	1.96	4.02	3.86 ^(c)
H ₁	5.32	10.00	9.96
H ₂	6.62	8.20	8.32

(a)_R = 2.9%; (b)_R = 2.8%; (c)_R = 1.5%.

TABLE XX

MINIMUM R VALUES (%) AND LANTHANIDE POSITIONS FOR BINARY COMBINATIONS OF
METHYLACRYLONITRILE MODELS 5-7 WITH SETS OF RELATIVE SLOPES,
NO RESTRAINT OF LANTHANIDE POSITION

	LIS Data Set											
	<u>5</u>				<u>6</u>				<u>7</u>			
	R	d	θ	Ω	R	d	θ	Ω	R	d	θ	Ω
Model 1-CH ₃	3.2	2.3Å	5°	120°	14.4	2.1Å	85°	84°	0.3	3.0Å	35°	110°
Model <u>cis</u> -2-methyl	6.0	3.5Å	0°	0°	22.6	3.1Å	35°	0°	2.8	2.3Å	0°	0°
Model <u>trans</u> -2-methyl	29.8	3.5Å	15°	0°	.73	2.8Å	15°	20°	23.9	2.0Å	50°	180°

TABLE XXI

MINIMUM R VALUES (%) FOR BINARY COMBINATIONS OF METHYLACRYLONITRILE
 MODELS 5-7 WITH SETS OF RELATIVE SLOPES, WITH COLLINEARITY RESTRAINT

	LIS Data Sets		
	5	6	7
Model 1-CH ₃	2.9	31.7	9.7
Model <u>cis</u> -2-CH ₃	6.0	26.6	2.8
Model <u>trans</u> -2-CH ₃	29.3	1.5	27.1
Ratio, $\frac{\text{Second best}}{\text{best}}$	2.06	17.7	3.46
Confidence level (%) for rejection of second best model	27 (73)	4 (96)	19 (81)

four pairs of isomeric cinnamitriles and have obtained results which support the assumption of a collinear lanthanide nitrile bond.

Cyanocyclopropane

Additional evidence which supports the assumption of a collinear nitrile lanthanide bond is the cyanocyclopropane system. The $^1\text{H-Yb}(\text{DPM})_3$ LIS indices for cyanocyclopropane were determined following the general procedure outlined in Appendix C. The set of relative slopes resulting from this LIS experiment can also be found in Appendix C. Table XXII contains the R factors and lanthanide positions obtained for these relative slopes. Note that without any restraints, a minimum R factor of 3.02 is found at a lanthanide position 10° off the axis of the nitrile bond. However the goodness of fit (R factor) seems to be a soft function of both the angular tilt off the nitrile axis and the bond length. Application of the collinearity restraint, yields the second set of R factors and bond distances in Table XXII. Again the goodness of fit seems to be a soft function of the lanthanide nitrogen bond distance. The two positions (linear and no restraint) corresponding to a best fit seem to be virtually identical.

Benzonitriles

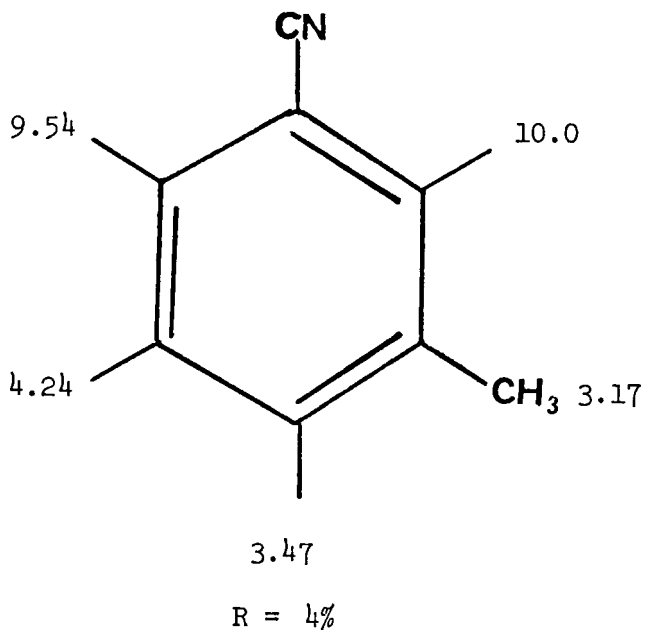
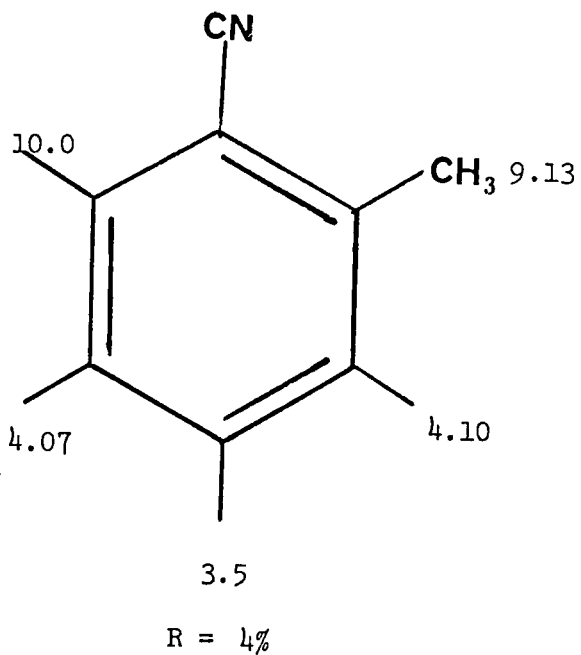
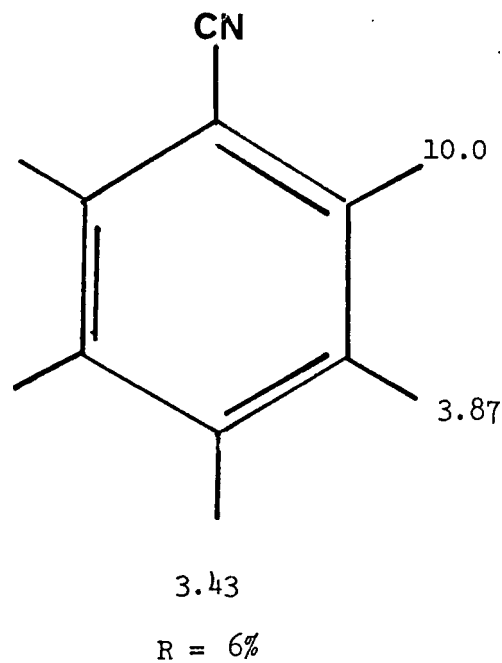
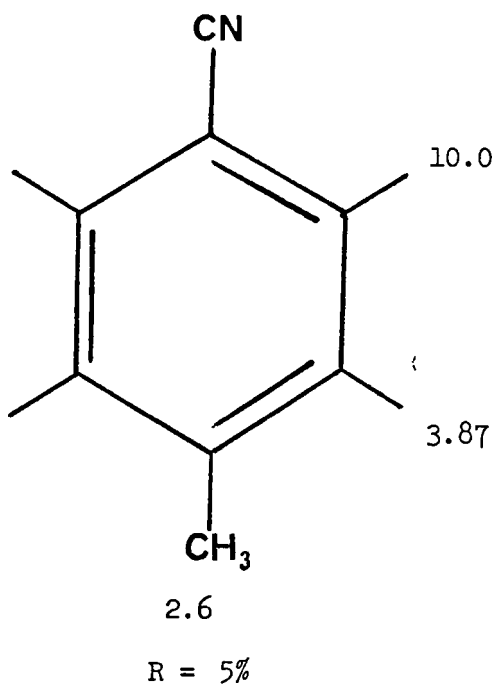
Four substituted benzonitriles also serve to make the case for the collinear nitrile lanthanide bond stronger. The four compounds along with the R factors for each appear in Figure 9. The R factors

TABLE XXII

THE VARIATION OF THE AGREEMENT FACTOR, R, WITH THE LANTHANIDE POSITION FOR THE CYANO-
CYCLOPROPANE $^1\text{H-Yb}(\text{DPM})_3$ SYSTEM

R (%)	No Restraint			Linear	
	d (Å)	θ°	Ω°	d (Å)	R (%)
4.30	1.8	10	264	1.8	5.15
4.21	1.9	10	264	1.9	4.62
4.04	2.0	10	144	2.0	4.19
3.85	2.1	0	0	2.1	3.85
3.61	2.2	0	0	2.2	3.61
3.46	2.3	0	0	2.3	3.46
3.40	2.4	0	0	2.4	3.40
3.34	2.5	10	96	2.5	3.41
3.20	2.6	10	72	2.6	3.49
3.05	2.7	10	24	1.7	3.54
3.02	2.8	10	24	2.8	3.61
3.14	2.9	10	24	2.5	3.76
3.13	3.0	20	30	3.0	3.85

FIGURE 9: THE OBSERVED $\text{Yb}(\text{DPM})_3$ -PROTON INDICES FOR FOUR
SUBSTITUTED BENZONITRILES WITH AGREEMENT FACTORS
FOR EACH



obtained for each compound is reasonable. Moreover the positions corresponding to a best fit are within 10° of the axis of the nitrile bond.

In summary, there is good evidence that the nitrile lanthanide bond is linear. The effect of this linearity is to make the statistics of the Willcott and Davis⁸⁷ kind of hypothesis testing more secure in all nitrile-containing substrates. In nitrile systems with a few number of observations, the removal of two of the parameters by the assumption of collinearity make hypothesis testing possible.

Conformational Analysis Using Nitrile-Containing Compounds

Willcott, Davis, Sachdev and Doering¹¹³ have studied the ring pucker of the cyclobutyl ring in cis and trans-1-cyano-2-vinylcyclobutane. The authors note that the ring pucker problem, in cyclobutane rings, should be reasonably approximated by a single minimum potential energy surface. The Yb-¹H LIS values for these two compounds were obtained in the usual way. The relative slopes for the cyclobutyl ring of these two compounds are shown in Figure 10. The agreement factors, R, for a variety of puckered cyclobutyl rings was computed. The extent of the ring pucker was measured as a dihedral angle about C₁ and C₄ defined in such a way that a positive dihedral angle made the cyano group more axial. The agreement factors were displayed as a function of this defined dihedral angle. These are graphically illustrated in Figures 11 and 12. The values displayed as the calculated values were the values calculated at the position of minimum R. Both curves are

FIGURE 10: THE OBSERVED $Y_b(\text{FOD})_3$ - ^1H INDICES FOR CIS AND
TRANS-1-CYANO-2-VINYLCYCLOBUTANE DETERMINED BY
DOERING (from reference 113)

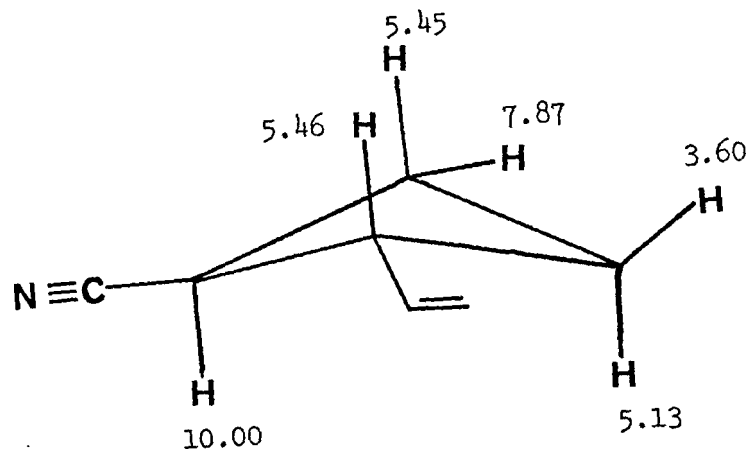
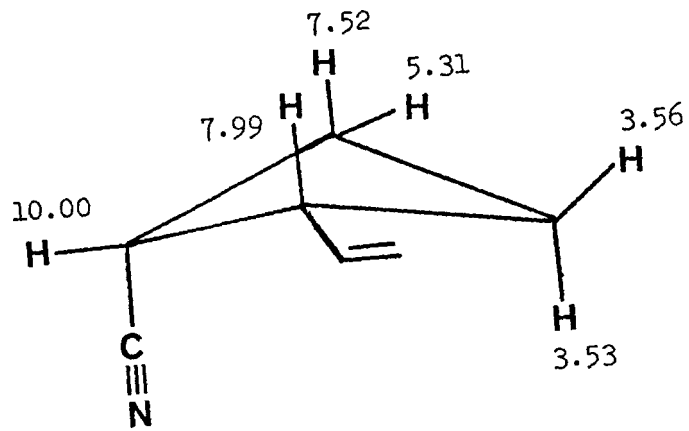
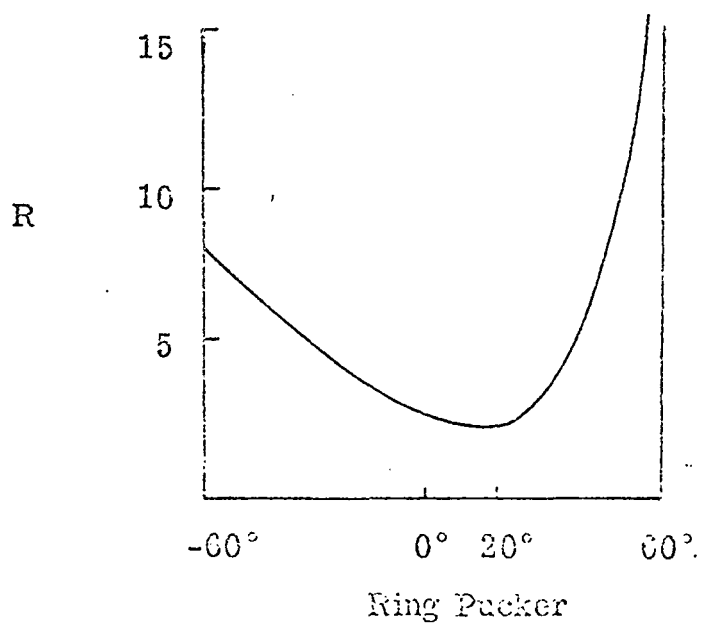
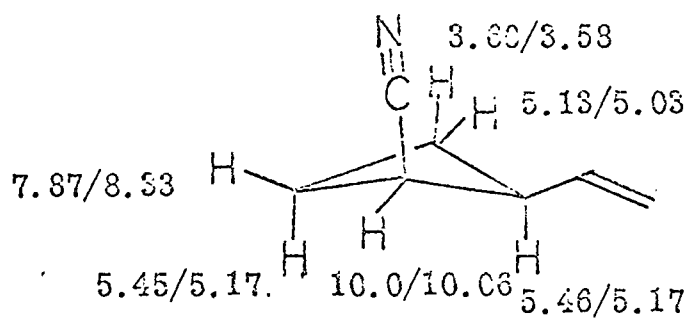
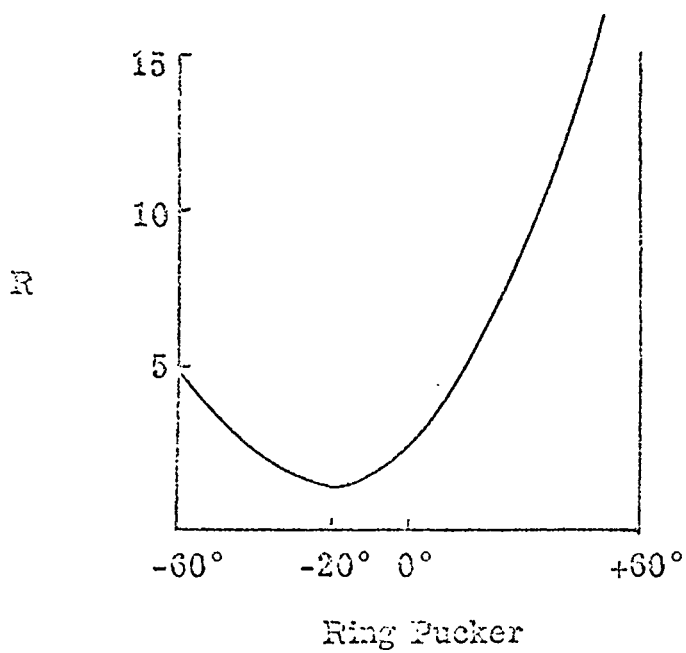
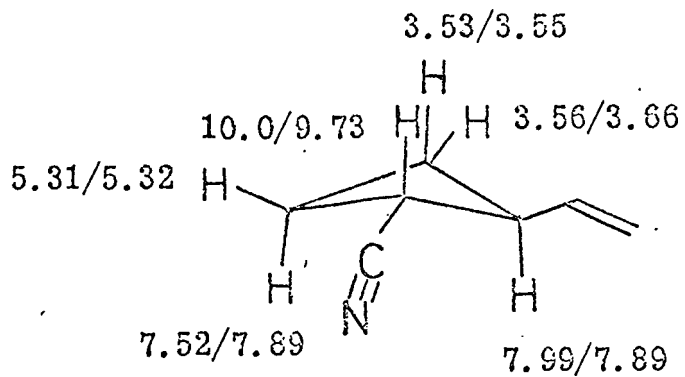


FIGURE 11: VARIATION OF THE AGREEMENT FACTOR, R , WITH RING
PUCKER IN THE CYCLOBUTYL RING OF CIS-1-CYANO-2-
VINYLCYCLOBUTANE (from reference 113)



Doering
 Sachdev
 Davis
 Willett

FIGURE 12: VARIATION OF THE AGREEMENT FACTOR, R , WITH THE RING
PUCKER IN THE CYCLOBUTYL RING OF TRANS-1-CYANO-2-
VINYL CYCLOBUTANE (from reference 113)



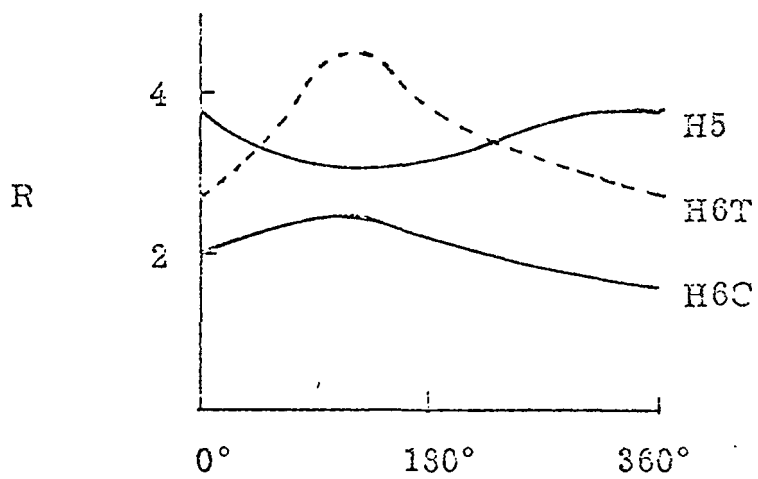
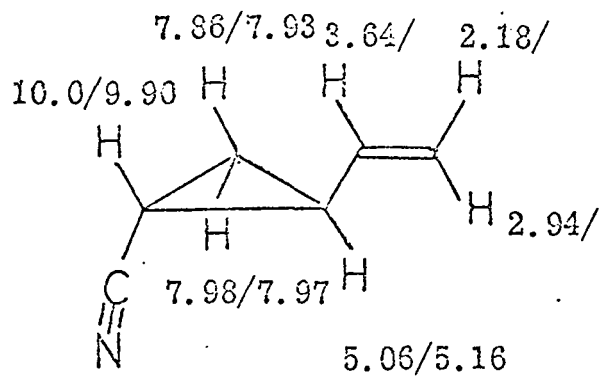
Doering
Sachdev
Davis
Wallcott

consistent with the notion that the ring pucker should be represented by a single minimum potential energy curve. The authors did not attempt to analyze the conformational problems concerning the vinyl group in these compounds.

Cooke, Lenkinski, Davis and Willcott¹¹⁴ have studied the conformation of the vinyl group in trans-1-cyano-2-vinylcyclopropane. The Yb-¹H LIS indices were determined by the standard procedure outlined in Appendix C. The relative slopes for the seven resonances were determined and are shown in Figure 13. The lanthanide position was determined using the four cyclopropyl resonances. The vinyl group was then rotated incrementally through 360° in the computer and at each angle an R factor determined. The variation of the agreement of each olefinic resonance was displayed as a function of θ , the angle of rotation. This variation is shown for each olefinic resonance in Figure 13. Interpretation of these curves is not obvious. A careful consideration of this problem indicates the complexity of the analysis.

The low temperature NMR experiment performed on vinylcyclopropane by De Mare and Martin,¹¹⁵ indicate that there are three conformational potential energy wells. At room temperature, the observed shifts are a time average of these three conformers. The populations of these three conformers are not known in the LIS experiment, at room temperature. The populations of the various conformers generate three more parameters that need to be determined. The fact

FIGURE 13: VARIATION OF THE AGREEMENT FACTOR, R , WITH THE ANGLE OF ROTATION OF THE VINYL GROUP FOR EACH OF THE OLEFINIC RESONANCES OF TRANS-1-CYANO-2-VINYLCYCLOPROPANE (from reference 114)



Cocke
 Lenkinski
 Davis
 Willcott

that so many parameters must be extracted from so few observable quantities make this kind of conformational analysis very difficult. However, the nitrile group still offers the advantage of reducing the number of parameters necessary to define the lanthanide location in the substrate systems. While preliminary attempts at solving the type of conformational problems involving potential energy surfaces with more than one minimum have met with little success, the computational method outlined, coupled with additional information from sources other than LIS experiments, can still provide at least qualitative answers to conformational problems.

CHAPTER VII

SUMMARY OF THE COMPUTATIONAL METHOD

VII. SUMMARY OF THE COMPUTATIONAL METHOD

In the statement of purpose, the question, "Can we determine the structure of substrate molecules from their LIS data?" was posed. In attacking this problem, we have discussed the following questions raised by Willcott and Davis.¹¹¹

- I. How can LIS indices best be determined?
- II. Should the observed shifts be factored into contact and pseudocontact contributions?
- III. Is the use of the McConnell-Robertson relationship for axially symmetric ions appropriate?
- IV. What orientation of the principal magnetic axis should be used for the computer simulation of the experiment?
- V. What is the optimum method for matching experimental and calculated LIS values?

We have presented chemical justification for some of the conclusions reached in our discussion of these topics. In some cases, however, we could not resolve the particular question under discussion on a purely chemical basis. In these cases, we chose to construct the simplest physical model for the LIS nmr experiment which still generated substrate structures consistent with other available chemical information. Some of the simplifying assumptions we have made in constructing this simplest model have come under considerable criticism.

For example, Horrocks¹¹ has cautioned against using the McConnell-Robertson relationship for axially symmetric ions. In describing the

structures of the $\text{Ln}(\text{DPM})_3$ LSRs he notes:

"In the solid state the complex is not even approximately axially symmetric. The present structure, while not necessarily the only one present in solution, is a likely contributor in the solution state for complexes of this type. Our results suggest that the assumption of axial symmetry for shift-reagent adducts in solution may not be strictly valid and structural inferences made on this basis must be accepted with reservation."

Perhaps a more subtle point has been raised by Randall¹⁴ and Marshall.¹⁵ These authors have constructed computational methods which have attempted to take into account the dynamic nature of the LSR-substrate complex. In our computational scheme, we have used a static description of the LSR-substrate complex. The lanthanide positions generated by our computational method, may be, for this reason, artifacts of our computation. However, in almost all cases, the position of the lanthanide generated by our method has been in a chemically reasonable location. In a summary of the computational scheme presented on page 57, we have noted that the agreement factor, R, is generally insensitive to the lanthanide location within $.1 \overset{\circ}{\text{Å}}$ in the bond length and $5\text{-}10^\circ$ in the angular coordinates. Our computational scheme is, for this reason, not a good method for generating precise lanthanide locations.

The method is sensitive to substrate topologies. Perhaps the strongest reply to any criticisms of the computational method we have developed, is the fact that, in all cases we have examined, the substrate structures generated by our method have been the "correct"

substrate structures. In describing the computational scheme

Willcott and Davis¹¹¹ note:

"We are convinced that the essential topology we have deduced will stand scrutiny even after the answers to the questions raised earlier have been assiduously evaluated. In the meantime we plan to pursue this method of structure determination because it is both rapid and quantitative. Of even more importance is the realization after solving more than 100 problems that we have learned new ways to think about the static and dynamic structures which are important in nmr experiments. Any method which produces this result is a success."¹¹¹

BIBLIOGRAPHY

BIBLIOGRAPHY

1. C. C. Hinckley, J. Amer. Chem. Soc., 91, 5160 (1969).
2. J. A. Jackson, J. F. Lemons and H. Taube, J. Chem. Phys., 32, 553 (1960).
3. R. E. Connick and D. N. Fiat, J. Chem. Phys., 39, 1349 (1963).
4. W. B. Lewis, J. A. Jackson, J. F. Lemons and H. Taube, J. Chem. Phys., 36, 694 (1965).
5. W. D. Phillips, C. E. Looney and C. K. Ikeda, J. Chem. Phys., 27, 1435 (1957).
6. D. R. Eaton, A. D. Josey, W. D. Phillips and R. E. Benson, J. Chem. Phys., 39, 3513 (1963).
7. D. R. Eaton, J. Amer. Chem. Soc., 87, 3097 (1965).
8. E. L. Muetterties and C. W. Wright, J. Amer. Chem. Soc., 87, 4706 (1965).
9. K. J. Eisentraut and R. E. Sievers, J. Amer. Chem. Soc., 87, 5254 (1965).
10. W. DeW. Horrocks, Jr. and J. P. Sipe III, J. Amer. Chem. Soc., 93, 6800 (1971).
11. W. DeW. Horrocks, Jr., J. P. Sipe III and J. R. Luber, J. Amer. Chem. Soc., 93, 5258 (1971).
12. A. R. Al-Karaghoulis and J. S. Wood, J. Amer. Chem. Soc., 90, 6548 (1968).
13. E. L. Muetterties and C. W. Wright, Quart. Rev. Chem. Soc., 21, 109 (1967).
14. G. P. Moss and E. W. Randall, Abstracts of the 165'th A.C.S. National Meeting, Dallas, Analytical, 47 (1973).
15. I. M. Armitage, L. D. Hall, A. G. Marshall and L. G. Werbelow, Abstracts of the 165'th A.C.S. National Meeting, Dallas, Analytical, 60 (1973).

16. C. S. Springer, D. W. Meek and R. E. Sievers, Inorg. Chem., 6, 1105 (1967).
17. J. K. M. Sanders and D. H. Williams, J. Amer. Chem. Soc., 93, 641 (1971).
18. H. Hart and G. M. Love, Tetrahedron Letters, 625 (1971).
19. L. Ernst and A. Mannschreck, Tetrahedron Letters, 3023 (1971).
20. W. L. F. Armarego, T. J. Batterham and J. R. Kershaw, Org. Mag. Resonance, 3, 575 (1971).
21. D. R. Eaton, W. D. Phillips and D. J. Caldwell, J. Amer. Chem. Soc., 85, 397 (1963).
22. K. D. Berlin and S. Rengaraju, J. Org. Chem., 36, 2912 (1971).
23. Z. W. Wolkowski, Tetrahedron Letters, 825 (1971).
24. J. M. J. Tronchet, F. Barbalat-Rey and N. Le-Hong, Helv. Chim. Acta, 54, 2615 (1971).
25. J. K. M. Sanders, S. W. Hanson and D. H. Williams, J. Amer. Chem. Soc., 94, 5325 (1972).
26. B. F. G. Johnson, J. Lewis, P. McArdle and J. R. Norton, Chem. Commun., 535 (1972).
27. R. A. Fletton, G. F. H. Green and J. E. Page, Chem. Ind., 167 (1972).
28. R. R. Fraser and Y. Y. Wigfield, Tetrahedron Letters, 2515 (1971).
29. R. E. Rondeau, M. A. Berwick, R. N. Steppel and M. P. Servé, J. Amer. Chem. Soc., 94, 1096 (1972).
30. C. Beauté, Z. W. Wolkowski and N. Thoai, Chem. Commun., 700 (1971).
31. A. H. Lewin, Tetrahedron Letters, 3583 (1971).
32. L. R. Isbrandt and M. T. Rogers, Chem. Commun., 1378 (1971).
33. T. M. Ward, I. L. Allcox and G. H. Wahl, Jr., Tetrahedron Letters, 4421 (1971).
34. K. K. Andersen and J. J. Uebel, Tetrahedron Letters, 5253 (1970).

35. R. R. Fraser and Y. Y. Wigfield, Chem. Commun., 1471 (1970).
36. R. A. Bauman, Tetrahedron Letters, 419 (1971).
37. W. Walter, R. F. Becker and J. Thiem, Tetrahedron Letters, 1971 (1971).
38. A. Kato and M. Numata, Tetrahedron Letters, 203 (1972).
39. Y. Kashman and O. Awerbouch, Tetrahedron, 27, 5593 (1971).
40. W. G. Bentrude, H. W. Tan and K. C. Yee, J. Amer. Chem. Soc., 94, 3264 (1972).
41. K. C. Yee and W. G. Bentrude, Tetrahedron Letters, 2775 (1971).
42. B. D. Cuddy, K. Treon and B. J. Walker, Tetrahedron Letters, 4433 (1971).
43. D. L. Rabenstein, Anal. Chem., 43, 1599 (1971).
44. F. J. Smentowski and R. D. Stipanovic, J. Amer. Oil Chem. Soc., 49, 48 (1972).
45. J. Paasivirta, Suomen Kemistilehti B, 44, 131 (1971).
46. J. Paasivirta, Suomen Kemistilehti B, 44, 135 (1971).
47. J. Paasivirta and P. J. Malkonen, Suomen Kemistilehti B, 44, 230 (1971).
48. Z. W. Wolkowski, Tetrahedron Letters, 821 (1971).
49. P. Kristiansen and T. Ledaal, Tetrahedron Letters, 2817 (1971).
50. J. Dale and P. Kristiansen, Chem. Commun., 670 (1971).
51. A. M. Grotens, J. Smid and E. De Boer, Tetrahedron Letters, 4863 (1971).
52. J. E. Herz, V. M. Rodriguez and P. Joseph-Nathan, Tetrahedron Letters, 2949 (1971).
53. D. F. Evans and W. Wyatt, Chem. Commun., 312 (1972).
54. R. C. Foster and C. A. Fyfe, Prog. in Nucl. Magn. Spectrosc., 4, 1 (1969).

55. B. L. Shapiro and M. D. Johnston, Jr., Abstracts of papers presented at the 13'th Experimental NMR Conference, 38 (1972).
56. A. Derenleau, J. Amer. Chem. Soc., 91, 4044,4050 (1969).
57. J. F. Desreux, L. E. Fox, and C. N. Reilley, Anal. Chem., 44, (1972).
58. T. J. Marks, R. Porter and D. F. Shriver, Proceedings of the Tenth Rare Earth Research Conference, Carefree, Arizona, I, 372 (1973).
59. G. Scatchard, Ann. N. Y. Acad. Sci., 51, 660 (1949).
60. K. Roth, M. Grosse and D. Rewicki, Tetrahedron Letters, 435 (1972).
61. P. V. Demarco, T. K. Elzey, R. B. Lewis and E. Wenkert, J. Amer. Chem. Soc., 92, 5734 (1970).
62. R. E. Rondeau and R. E. Sievers, J. Amer. Chem. Soc., 93, 1522 (1971).
63. D. R. Kelsey, J. Amer. Chem. Soc., 94, 1764 (1972).
64. M. R. Willcott, J. F. M. Oth, J. Thio, G. Plinke and G. Schroder, Tetrahedron Letters, 1579 (1971).
65. I. Armitage, G. Dunsmore, L. D. Hall and A. G. Marshall, Chem. Commun., 1281 (1971).
66. J. W. ApSimon and H. Bierbeck, Chem. Commun., 172 (1972).
67. E. Goerland, Masters Thesis, University of Houston, May 1973.
68. H. M. McConnell and R. E. Robertson, J. Chem. Phys., 29, 1361 (1958).
69. J. Reuben and D. Fiat, J. Chem. Phys., 51, 4909 (1969).
70. R. G. Shulman and S. Sugano, Phys. Rev., 130, 506 (1963).
71. Z. Luz and G. Shulman, J. Chem. Phys., 43, 3750 (1965).
72. J. Briggs, F. A. Hart, G. P. Moss and E. W. Randall, Chem. Commun., 364 (1971).
73. G. N. LaMar, W. DeW. Horrocks, Jr., and L. C. Allen, J. Chem. Phys., 41, 2126 (1964).

74. B. A. Goodman and J. B. Raynor, Advan. Inorg. Chem. Radiochem., 13, 135 (1970).
75. J. Briggs, F. A. Hart and G. P. Moss, Chem. Commun., 1506 (1971).
76. S. Farid, A. Ateya and M. Maggio, Chem. Commun., 1285 (1971).
77. C. D. Barry, A. C. T. North, J. A. Glasel, R. J. P. Williams, and A. V. Xavier, Nature, 232, 236 (1971).
78. R. Caple and S. C. Kuo, Tetrahedron Letters, 4413 (1971).
79. J. Reuben and J. S. Leigh, Jr., J. Amer. Chem. Soc., 94, 2789 (1972).
80. E. R. Brinbaum and T. Moeller, J. Amer. Chem. Soc., 91, 7274 (1969).
81. J. Reuben, Private communication.
82. W. DeW. Horrocks, Jr. and J. P. Sipe III, Science, 177, 994 (1972).
83. J. J. Uebel and R. M. Wing, J. Amer. Chem. Soc., 94, 8910 (1972).
84. G. E. Hawkes, C. Marzin, D. Liebfritz, S. R. Johns, K. Herwig, R. A. Cooper, D. W. Roberts and J. D. Roberts, Abstracts of the 165'th A.C.S. National Meeting, Dallas, Analytical, 043 (1973).
85. L. E. Ford, C. M. Dobson and R. J. P. Williams, Abstracts of the 165'th A.C.S. National Meeting, Dallas, Analytical, 046 (1973).
86. M. R. Willcott III, R. E. Lenkinski and R. E. Davis, J. Amer. Chem. Soc., 94, 1742 (1972).
87. R. E. Davis and M. R. Willcott, J. Amer. Chem. Soc., 94, 1744 (1972).
88. J. K. Sanders and D. H. Williams, Tetrahedron Letters, 2813 (1971).
89. C. C. Hinckley, M. R. Klotz and F. Patil, J. Amer. Chem. Soc., 93, 2417 (1971).
90. H. Huber and C. Pascual, Helv. Chim. Acta, 54, 913 (1971).
91. P. V. Demarco, B. J. Cerimele, R. W. Crane and A. L. Thakkar, Tetrahedron Letters, 3539 (1972).

92. N. S. Angerman, S. S. Danyluk, and T. A. Victor, J. Amer. Chem. Soc., 94, 7137 (1972).
93. J. A. Steers, "An Introduction to the Study of Map Projections," University of London Press, London, 1965.
94. W. C. Hamilton, "Statistics in Physical Science," Ronald Press, New York, N. Y., 1964, pp. 157-162.
95. W. C. Hamilton, Acta Crystallogr., 18, 502 (1965).
96. S. I. Weissman, J. Amer. Chem. Soc., 93, 4928 (1971).
97. O. A. Gansow, M. R. Willcott and R. E. Lenkinski, J. Amer. Chem. Soc., 93, 4295 (1971).
98. G. E. Hawkes, C. Marzin, S. R. Johns and J. D. Roberts, J. Amer. Chem. Soc., 95, 0000 (1973).
99. R. J. Cushley, D. R. Andersen and S. R. Lipsky, Chem. Commun., 636 (1972).
100. J. Reuben, "Paramagnetic Lanthanide Shift Reagents in NMR Spectroscopy; Principles, Methodology and Application," to appear in Progress in Nuclear Magnetic Resonance Spectroscopy, 1973.
101. M. Witanowski, L. Stefaniak, H. Januszewski and Z. W. Wolkowski, Tetrahedron Letters, 1653 (1971).
102. I. Morishima, K. Okada and T. Yonezawa, J. Amer. Chem. Soc., 94, 1425 (1972).
103. D. Doddrell and J. D. Roberts, J. Amer. Chem. Soc., 92, 6839 (1970).
104. R. E. Watson and A. J. Freeman, Phys. Rev. Letters, 6, 277 (1961).
105. W. D. Horrocks and D. L. Johnson, Inorg. Chem., 10, 1838 (1971).
106. M. J. Scarlett, A. T. Casey and R. A. Craig, Aust. J. Chem., 23, 1333 (1970).
107. R. Drago and R. E. Cramer, J. Amer. Chem. Soc., 92, 66 (1970).
108. O. A. Gansow, P. A. Loeffler, R. E. Davis, M. R. Willcott III and R. E. Lenkinski, J. Amer. Chem. Soc., 95, 3389 (1973).

109. O. A. Gansow, P. A. Loeffler, R. E. Davis, M. R. Willcott III and R. E. Lenkinski, J. Amer. Chem. Soc., 95, 3390 (1973).
110. M. R. Willcott III, R. E. Davis and P. A. Loeffler, unpublished results.
111. M. R. Willcott III and R. E. Davis, Proceedings of the Tenth Rare Earths Research Conference, Carefree, Arizona, I, 410 (1973).
112. R. Seux, G. Morel and A. Foucaud, Tetrahedron Letters, 1003 (1972).
113. W. Von E. Doreing, M. R. Willcott III and R. E. Davis, unpublished results.
114. M. R. Willcott III, R. E. Lenkinski, R. E. Davis and R. S. Cooke, unpublished results.
115. G. R. De Mare and J. S. Martin, J. Amer. Chem. Soc., 88, 5033 (1966).

APPENDIX A

$\text{Eu}(\text{DPM})_3$ LIS DATA FOR SOME RIGID BICYCLIC
OXYGENATED HYDROCARBONS

Eu(DPM)₃ LIS DATA FOR SOME RIGID BICYCLIC
OXYGENATED HYDROCARBONS

For the sake of completeness, the LIS data obtained for the rigid oxygenated hydrocarbons referred to in previous sections are recorded in this Appendix.

A general procedure for obtaining this ¹H data is presented along with two examples which illustrate the method. The compounds investigated are;

- (1) Borneol
- (2) Isoborneol
- (3) Norcamphor
- (4) endo-Norborn-5-en-2-ol
- (5) Bicyclo[3.2.0]hept-3-en-2-one
- (6) 5-Methylbicyclo[3.2.0]hept-3-en-2-one

A procedure for obtaining ¹³C-LIS indices is presented along with the ¹³C-LIS data for;

- (1) Isoborneol
- (2) Borneol

The General Experimental Procedure for Obtaining ¹H LIS Indices

In general, a stock solution, containing 200 mg of substrate in 5 mls CCl₄, with small amounts of TMS and chloroform, was prepared. All reagents and solvents were dried carefully before use. A 100 MHz ¹H spectrum of 0.5 mls of this stock solution was obtained on a Varian HA100 NMR Spectrometer. Sequential additions of Eu(DPM)₃* were made

*Prepared by the Sievers⁹ method.

in the following order; 10 mg, 10 mg, 20 mg, 20 mg, 40 mg of $\text{Eu}(\text{DPM})_3$. After each addition, a ^1H 100 MHz spectrum was again obtained. The resonances in each spectrum were measured relative to CHCl_3 as standard. Linear least squares refinement of δ_{obs} against mole ratio of $\text{Eu}(\text{DPM})_3/\text{substrate}$ yielded the slopes indicated for each compound. The two compounds obtained from Robert L. Cargill at the University of South Carolina can serve to illustrate the method.

5-Methylbicyclo[3.2.0]hept-3-en-2-one

The general procedure was followed to obtain the ^1H LIS indices for 5-methylbicyclo[3.2.0]hept-3-en-2-one. The experimental data for this compound can be found in Table XXIII.

Bicyclo[3.2.0]hept-3-en-2-one

The ^1H $\text{Eu}(\text{DPM})_3$ indices for this compound were determined using the general procedure outlined before. The experimental results for this compound can be found in Table XXIV.

TABLE XXIII

EXPERIMENTAL $\text{Eu}(\text{DPM})_3$ LIS DATA FOR 5-METHYLBICYCLO[3.2.0]HEPT-3-EN-2-ONE

Mole ratio $\text{Eu}(\text{DPM})_3/\text{substrate}$	Resonance ^(a)						
	H_1	H_2	H_3	H_4	H_5	H_6, H_7	CH_3
.0875	698	765	325	277	226	226	144
.175	773	797	443	317	291	239	171
.263	848	830	547	357	341	280	197
.350	937	863	654	387	429	315	225
.438	1011	903	773	435	495	347	254
.526	1101	936	907	485	585	383	282
Slope ^(b)	9.19	3.93	13.1	4.67	8.19	3.77	3.15

(a) All resonances are given in Hz from TMS.

(b) The slopes are given in ppm.

TABLE XXIV

EXPERIMENTAL LIS DATA FOR BICYCLO[3.2.0]HEPT-3-EN-2-ONE

Mole ratio Eu(DPM) ₃ /substrate	Resonance ^(a)							
	H ₁	H ₂	H ₃	H ₄	H ₅	H ₆	H ₇	H ₉
.0782	782	681	358	358	272	258	218	190
.156	808	751	450	404	310	292	274	218
.234	836	836	550	446	342	306	342	250
.312	870	908	652	488	382	338	404	276
.391	902	988	760	536	424	370	478	310
.469	939	1097	890	529	470	402	560	341
Slope ^(b)	4.04	10.51	13.5	5.89	5.03	3.64	8.7	4.00

(a) All resonances are given in Hz from TMS.

(b) The slopes are given in ppm.

The same general procedure was followed to obtain the ^1H indices for the remaining compounds. All numbers are in ppm units.

Borneol:

H_2	H_{3x}	H_{3n}	H_4	H_{5x}	H_{5n}	H_{6x}	H_{6n}
25.5	8.8	16.7	5.1	5.1	7.0	7.4	17.5
		$(\text{CH}_3)_{10}$		$(\text{CH}_3)_{\text{syn}}$		$(\text{CH}_3)_{\text{anti}}$	
		8.6		4.4		4.0	

Note n means endo, x means exo, syn means syn with respect to the hydroxyl group and anti means anti with respect to the hydroxyl group.

Isoborneol:

H_2	H_{3x}	H_{3n}	H_4	H_{5x}	H_{5n}	H_{6x}	H_{6n}
26.7	19.2	9.3	6.7	4.5	3.5	5.1	7.2
		$(\text{CH}_3)_{10}$		$(\text{CH}_3)_{\text{syn}}$		$(\text{CH}_3)_{\text{anti}}$	
		10.5		11.0		4.7	

Norcamphor:

H_1	H_{3x}	H_{3n}	H_4	H_{5x}	H_{5n}	H_{6x}	H_{6n}	$\text{H}_{7\text{syn}}$	$\text{H}_{7\text{anti}}$
11.8	13.6	14.4	4.4	3.9	4.4	4.4	6.2	8.0	4.7

endo-Norborn-5-en-2-ol:

H ₁	H ₂	H _{3x}	H _{3n}	H ₄	H ₅	H ₆	H _{7syn}	H _{7anti}
10.5	23.0	8.35	12.8	4.9	6.9	8.8	8.4	4.9

The Experimental Procedure for Determining the ^{13}C LIS Indices for Borneol

5 mls of 1.0 M solution of borneol in CCl_4 containing hexafluorobenzene and TMS as internal standards were prepared. A ^{13}C spectrum of this solution was taken on a Bruker HFX-90* equipped with a pulsed FFT system. Sequential additions of $\text{Eu}(\text{DPM})_3$ were made to this solution in such a way that the mole ratio of $\text{Eu}(\text{DPM})_3$ /substrate was approximately 0.1, 0.3, 0.4, and 0.5. After each addition, a ^{13}C spectrum was obtained. In each spectrum, the position of each resonance was measured relative to internal TMS. Linear least squares refinement of the resonance position $\delta_{i(\text{obs})}$ in each spectrum against the mole ratio of $\text{Eu}(\text{DPM})_3$ /borneol yielded the ^{13}C LIS parameters for borneol.

Borneol ^{13}C LIS Data

C_1	C_2	C_3	C_4	C_5	C_6	C_7	C_8	C_9	C_{10}
13.9	55.0	20.0	10.0	11.4	14.9	9.1	4.4	6.6	13.6

Isoborneol ^{13}C LIS Data

C_1	C_2	C_3	C_4	C_5	C_6	C_7	C_8	C_9	C_{10}
9.8	39.8	15.8	7.6	5.0	5.6	7.4	4.2	10.0	11.4

*The Bruker HFX-90 was made available by O. A. Gansow at Rice University.

APPENDIX B

GENERAL PROCEDURE FOR OBTAINING A SET OF MATCHED ^{13}C AND
 ^1H LIS INDICES FOR A COMPOUND

GENERAL PROCEDURE FOR OBTAINING A SET OF MATCHED ^{13}C AND
 ^1H LIS INDICES FOR A COMPOUND

The liquid substrates used were all dried over molecular sieve for a period of three days before use. All the LSRs were prepared following the general method outlined by Sievers.⁹ The crude lanthanide chelates were recrystallized twice from dry hexane. The recrystallized chelates were then dried under vacuum over P_2O_5 overnight before use. In all transfers of either substrates or LSRs, precautions to maintain the dryness of the compounds were taken.

50 mls of a 1.0 M solution of the substrate were prepared in CCl_4 containing hexafluorobenzene as a lock signal, CHCl_3 and TMS as an internal standard. A ^{13}C spectrum of this solution was obtained on a Bruker HFX-90 equipped with a pulsed FFT system. Usually 1024 or 2048 pulses were taken for each spectrum. 0.5 ml of this solution was transferred into a 5 mm nmr tube and the ^1H spectrum for this sample was taken on a Varian HA100. Sequential additions of LSR were made to this solution in such a way that the mole ratio of the LSR/substrate obtained was 0.1, 0.2, 0.3, 0.4, 0.5 and 0.6. After each addition, a ^{13}C spectrum was obtained. After each addition, a ^1H spectrum was also obtained. In both cases, the positions of each resonance were determined relative to either TMS or CHCl_3 . Linear least squares refinement of the resonance position (δ_{ppm}) against the mole ratio of LSR/substrate provide a set of slopes which were taken to be the ^1H and ^{13}C LIS indices for the particular substrate in question.

The results of using this procedure for $\text{Eu}(\text{DPM})_3$ as LSR and six pyridine type bases as substrates are shown in Table IX. The results of using the procedure for eight various LSRs and isoquinoline as substrate are given in Table X.

APPENDIX C

^1H Yb(DPM) $_3$ -LIS DATA FOR SOME NITRILE CONTAINING SUBSTRATES

^1H Yb(DPM)₃-LIS DATA FOR SOME NITRILE CONTAINING SUBSTRATES

A general procedure for obtaining ^1H indices for nitrile containing substrates is presented along with several illustrative examples of the method.

General Experimental Procedure for Obtaining ^1H Yb(DPM)₃-LIS Data for Nitrile Containing Substrates

In general about 200 mg of substrate was dissolved in 5 mls of CCl_4 containing TMS and CHCl_3 as internal standards. A ^1H spectrum of 0.5 mls of this solution was obtained on a Varian HA100. Approximately six sequential additions of Yb(DPM)_3 were made to the .5 mls of this solution. After each addition, a 100 MHz spectrum was obtained. The resonance position in each spectrum was measured relative to TMS as internal standard. The ApSimon method of data treatment was used to generate LIS indices. That is, the resonance position of each type of proton (ν_i) was plotted against the sum of resonance positions in each spectrum, $\sum \nu_i$, and the slope of this plot was obtained. These slopes are a set of relative LIS indices. One of Doering's Feist's acid derivatives (E-trans) and cyanocyclopropane can serve to illustrate the method. The data for these molecules are presented in Tables XXV and XXVI respectively.

TABLE XXV

 ^1H Yb(DPM)₃-LIS DATA FOR STRUCTURE E-TRANS

Yb(DPM) ₃ Additions	Resonance					Σv_i
	H _{gem}	H _{cis}	H _{olefin}	CH ₃	(CH ₃) _{olefin}	
0	142	198	602	124	184	1250
I	212	252	632	144	196	1446
II	350	360	696	194	224	1824
III	486	462	756	242	254	2200
IV	614	560	814	282	282	2552
Slope	.359	.278	.163	.124	.076	
Slope scaled to H _{gem} = 10 ppm	10.0	7.74	4.54	3.45	2.15	

(a) Resonances are in Hz from TMS.

TABLE XXVI

 ^1H Yb(DPM)₃-LIS DATA FOR CYANOCYCLOPROPANE

Yb(DPM) ₃ Additions	Resonance Positions (ν_i) ^(a)			$\Sigma \nu_i$
	H _{gem}	H _{cis}	H _{trans}	
I	186	144	124	454
II	250	204	168	620
III	434	348	266	1048
IV	468	376	288	1132
Slope	.413	.345	.242	
Slope scaled to H _{gem} = 10 ppm		8.35	5.85	

(a) The resonances are measured in Hz relative to TMS. H_{gem} is the proton geminal to the cyano group. H_{trans} is the proton trans to the cyano group and H_{cis} is the proton cis to the cyano group.